รายงานวิจัยฉบับสมบูรณ์

โครงการ

การพัฒนาตัวเร่งปฏิกิริยาแบบวิวิธภัณฑ์สำหรับใช้ในการผลิตสารเคมีมูลค่าเพิ่มสูง

โดย

ผศ.ดร. จูงใจ ปั้นประณต และคณะ

พฤษภาคม 2550

สัญญาเลขที่ MRG 48-80177

รายงานวิจัยฉบับสมบูรณ์

โครงการ

การพัฒนาตัวเร่งปฏิกิริยาแบบวิวิธภัณฑ์สำหรับใช้ในการผลิตสารเคมีมูลค่าเพิ่มสูง

คณะผู้วิจัย

1) ผศ.ดร. จูงใจ ปั้นประณต

สังกัด

ภาควิชาวิศวกรรมเคมี คณะวิศวกรรมศาสตร์

จุฬาลงกรณ์มหาวิทยาลัย

2) ศ.ดร. ปิยะสาร ประเสริฐธรรม

ภาควิชาวิศวกรรมเคมี คณะวิศวกรรมศาสตร์

จุฬาลงกรณ์มหาวิทยาลัย

สนับสนุนโดยสำนักงานคณะกรรมการอุดมศึกษาและสำนักงานกองทุนสนับสนุนการวิจัย

Abstract

Selective hydrogenation of acetylenic compounds over a series of supported Pd catalysts has been studied in both gas-phase and liquid-phase. The effects of catalyst composition, preparation method, as well as the type of solvent used were extensively investigated. For the use of TiO_2 support, acetylene conversions were found to be merely dependent on Pd dispersion while ethylene selectivity appeared to be strongly affected by the presence of Ti^{3+} in the TiO_2 samples. For the use of SiO_2 support, palladium silicide was formed on the sol-gel derived SiO_2 supported Pd catalysts when they were prepared by ion-exchange method using $Pd(NH_3)_4Cl_2$ as a palladium precursor. The Pd/SiO_2 catalysts with Pd silicide formation were found to exhibit superior performance than commercial SiO_2 supported ones in liquid-phase semihydrogenation of phenylacetylene. From XPS results, the binding energy of Pd 3d of palladium silicide on the Pd/SiO_2 catalyst shifted toward larger binging energy, indicating that Pd is electron deficient. This could probably result in an inhibition of a product styrene on the Pd surface. Liquid phase hydrogenation of cyclohexene under mild conditions on Pd/SiO_2 in different organic solvents (benzene, heptanol, and NMP), under pressurized carbon dioxide, and under solvent less condition were also investigated and compared. Hydrogenation rates were much higher when the reactions were performed under high pressure CO_2 or under solvent less condition. The use of high pressure CO_2 can probably enhance H_2 solubility in the substrate resulting in a higher hydrogenation activity. However, metal sintering and leaching in the presence of high pressure CO_2 were comparable to those in organic solvents.

Keywords selective acetylene hydrogenation, phenylacetylene hydrogenation, cyclohexene hydrogenation, supported Pd catalyst, Pd/TiO_2, Pd/SiO_2

บทคัดย่อ

งานวิจัยนี้ศึกษาปฏิกิริยาไฮโดรจิเนชันแบบเลือกเกิดของสารอัลไคน์เป็นอัลคีนโดยตัวเร่งปฏิกิริยาแพลเลเดียมบนตัวรองรับต่าง ๆในวัฏภาคของเหลวและวัฏภาคแก๊ส โดยเน้นถึงปัจจัยต่าง ๆที่มีผลต่อประสิทธิภาพของตัวเร่งปฏิกิริยาเช่นองค์ประกอบของตัวเร่งปฏิกิริยา วิธีการสังเคราะห์ตัวเร่งปฏิกิริยาและชนิดของตัวทำละลายที่ใช้ในวัฏภาคของเหลว เป็นต้น ในการใช้ไทเทเนียมไดออกไซด์เป็นตัวรองรับพบว่าอัตราการเกิดปฏิกิริยาในปฏิกิริยาไฮโดรจิเนชันของอะเซทิลีนในวัฏภาคแก๊สขึ้นอยู่กับการกระจายตัวของโลหะแพลเลเดียม ในขณะที่การเลือกเกิดเป็นผลิตภัณฑ์ที่ต้องการ(เอทิลีน)ขึ้นอยู่กับปริมาณ Ti^{3+} ที่อยู่บนตัวรองรับไทเทเนียมไดออกไซด์ ส่วนการใช้ซิลิกาเป็นตัวรองรับพบว่าเกิดสารประกอบแพลเลเดียมซิลิไซด์ขึ้นถ้าเตรียมซิลิกาโดยวิธีโซล-เจลและใช้วิธีการแลกเปลี่ยนไอออนในการเตรียมตัวเร่งปฏิกิริยาโดยใช้ $Pd(NH_3)_4Cl_2$ เป็นสารตั้งต้น อย่างไรก็ตามตัวเร่งปฏิกิริยาที่เกิดสารประกอบดังกล่าวให้ประสิทธิภาพดีกว่าตัวเร่งปฏิกิริยาแพลเลเดียมที่เตรียมบนซิลิกาเกรดการค้าในปฏิกิริยาไฮโดรจิเนชันแบบเลือกเกิดของฟีนิลอะเซทิลีนเป็นสไตรีนในวัฏภาคของเหลว จากการวิเคราะห์ด้วยเทคนิคเอ็กซเรย์โฟโตอิเลคตรอนสเปกโตรสโกปี พบว่าค่าพลังงานของ Pd 3d ในแพลเลเดียมซิลิไซด์มีค่ามากกว่าปกติแสดงถึงการขาดอิเลคตรอน ซึ่งอาจส่งผลให้สมบัติทางไฟฟ้าของพื้นผิวของแพลเลเดียมเปลี่ยนแปลงไปทำให้การดูดซับของสไตรีนลดลงส่งผลให้เกิดผลิตภัณฑ์ที่ต้องการมากขึ้น ในการเปรียบเทียบผลของตัวทำละลายอินทรีย์ต่าง ๆอาทิ เบนซีน เฮปทานอล และ นอร์มัลไพโรลิโดน กับการใช้คาร์บอนไดออกไซด์วิกฤติยิ่งยวดแทนตัวทำละลาย ในปฏิกิริยาไฮโดรจิเนชันของไซโคลเฮกซีนในวัฏภาคของเหลว พบว่าอัตราการเกิดปฏิกิริยาสูงขึ้นเมื่อใช้คาร์บอนไดออกไซด์วิกฤติยิ่งยวดเนื่องมากจากแก๊สไฮโดรเจนสามารถละลายได้ดีในคาร์บอนไดออกไซด์วิกฤติยิ่งยวดมากกว่าในตัวทำละลายอินทรีย์อย่างไรก็ตามพบการเสื่อมสภาพของตัวเร่งปฏิกิริยาแพลเลเดียมเช่นการซินเทอริงและการถูกชะล้างของโลหะแพลเลเดียมในปริมาณที่ใกล้เคียงกัน

คำสำคัญ ปฏิกิริยาไฮโดรจิเนชัน อะเซทิลีน ฟีนิลอะเซทิลีน ไซโคลเฮกซีน ตัวเร่งปฏิกิริยาแพลเลเดียม ไทเทเนียมไดออกไซด์ ซิลิกา

Executive Summary

การผลิตสารเคมีมูลค่าเพิ่มสูงโดยทั่วไปกระบวนการผลิตแบบดั้งเดิมใช้วิธีการสังเคราะห์ทางเคมีโดยไม่ใช้ตัวเร่งปฏิกิริยาอาทิการผลิตโพรพิลีนไกลคอลซึ่งเป็นสารเคมีที่ใช้ในอุตสาหกรรมอาหารและเครื่องใช้ต่างๆ การผลิตเชิงพาณิชย์ใช้กระบวนการไฮเดรชันของโพรพิลีนออกไซด์ซึ่งมีขั้นตอนการเกิดปฏิกิริยาหลายขั้นตอนและมีการใช้สารไฮโดรเจนเปอร์ออกไซด์ซึ่งเป็นสารอันตราย ในกระบวนการดังกล่าวนอกจากผลิตภัณฑ์ที่ต้องการแล้วจะเกิดสารอื่นๆที่ไม่ต้องการและเป็นมลพิษต่อสิ่งแวดล้อมอีกปริมาณมากที่จะต้องกำจัดทิ้งเช่นตัวทำละลาย สารประกอบเกลือ และผลิตภัณฑ์ข้างเคียงอื่นๆ ในปัจจุบันมีความสนใจอย่างมากในการเปลี่ยนกระบวนการสังเคราะห์สารเคมีมูลค่าเพิ่มสูงโดยวิธีการใช้ตัวเร่งปฏิกิริยาแบบวิวิธภัณฑ์ ข้อดีของวิธีดังกล่าวคือลดการใช้และการเกิดสารอันตรายที่ไม่ต้องการ ลดต้นทุนการผลิตและเพิ่มประสิทธิภาพของกระบวนการผลิต ไม่นานมานี้ได้มีงานวิจัยนำเสนอการผลิตโพรพิลีนไกลคอลจากกรดแลคติกโดยใช้ตัวเร่งปฏิกิริยารูเทเนียมบนถ่านกัมมันต์เป็นตัวเร่งปฏิกิริยาให้ผลการสังเคราะห์เป็นที่น่าพอใจตัวอย่างปฏิกิริยาอื่นๆที่สามารถเกิดปฏิกิริยาบนตัวเร่งปฏิกิริยาแบบวิวิธพันธ์ได้แก่ ปฏิกิริยาไฮโดรจิเนชันของสารอะโรมาติก ปฏิกิริยาไฮโดรจิเนชันแบบเลือกเกิดของสารอัลไคน์และอัลคีน ปฏิกิริยาเมตาเทซิสของโอเลฟินส์ ปฏิกิริยาอัลคิลเลชันของสารประกอบเอมีนและแอลกอฮอล์ เป็นต้น

อย่างไรก็ตามในการประยุกต์ใช้ตัวเร่งปฏิกิริยาในการสังเคราะห์สารเคมีมูลค่าเพิ่มสูงยังมีข้อจำกัดอยู่มาก เช่น ประสิทธิภาพที่ต่ำของตัวเร่งปฏิกิริยาทั้งด้านความว่องไวในการเกิดปฏิกิริยา ความสามารถในการเลือกเกิดปริมาณการผลิตและเสถียรภาพของตัวเร่งปฏิกิริยาทำให้ต้องมีการค้นหาหรือพัฒนาตัวเร่งปฏิกิริยาที่มีประสิทธิภาพสูงสำหรับใช้ในแต่ละปฏิกิริยาต่อไปนอกจากนี้ยังมีข้อจำกัดในเรื่องของสารตั้งต้นที่จำเป็นต้องมีความบริสุทธิ์สูงเพื่อป้องกันการเสื่อมสภาพของตัวเร่งปฏิกิริยาและการควบคุมสภาวะในการเกิดปฏิกิริยา การศึกษาวิจัยถึงปัจจัยอื่นๆที่มีผลต่อประสิทธิภาพและการเสื่อมสภาพของตัวเร่งปฏิกิริยาอาทิ สารตั้งต้นที่ใช้ สภาวะที่ใช้ในการทำปฏิกิริยาจึงมีความจำเป็นเป็นอย่างยิ่งเพื่อให้สามารถวางแผนการผลิตสารเคมีมูลค่าเพิ่มสูงโดยใช้ตัวเร่งปฏิกิริยาแบบวิวิธพันธ์ได้อย่างมีประสิทธิภาพ นอกจากนี้ การประยุกต์ใช้ตัวทำละลายที่ไม่เป็นพิษต่อสิ่งแวดล้อมเช่นคาร์บอนไดออกไซด์วิกฤติยิ่งยวด (Supercritical CO_2) และตัวเร่งปฏิกิริยาแบบวิวิธพันธ์ เป็นการพัฒนากระบวนการผลิตสารเคมีโดยไม่เป็นพิษต่อสิ่งแวดล้อมอย่างแท้จริง (Green chemistry)

งานวิจัยนี้พบว่าอัตราการเกิดปฏิกิริยาในปฏิกิริยาไฮโดรจิเนชันของอะเซทิลีนในวัฏภาคแก๊สโดยตัวเร่งปฏิกิริยาแพลเลเดียมบนไทเทเนียมไดออกไซด์ขึ้นอยู่กับการกระจายตัวของโลหะแพลเลเดียม ในขณะที่การเลือกเกิดเป็นผลิตภัณฑ์ที่ต้องการ(เอทิลีน)ขึ้นอยู่กับปริมาณ Ti^{3+} ที่อยู่บนตัวรองรับไทเทเนียมไดออกไซด์ ส่วนการใช้ซิลิกาเป็นตัวรองรับพบว่าเกิดสารประกอบแพลเลเดียมซิลิไซด์ขึ้นถ้าเตรียมซิลิกาโดยวิธีโซล-เจลและใช้วิธีการแลกเปลี่ยนไอออนในการเตรียมตัวเร่งปฏิกิริยาโดยใช้ $Pd(NH_3)_4Cl_2$ เป็นสารตั้งต้นอย่างไรก็ตามตัวเร่งปฏิกิริยาที่เกิดสารประกอบดังกล่าวให้ประสิทธิภาพดีกว่าตัวเร่งปฏิกิริยาแพลเลเดียมที่เตรียมบนซิลิกาเกรดการค้าในปฏิกิริยาไฮโดรจิเนชันแบบเลือกเกิดของฟีนิลอะเซทิลีนเป็นสไตรีนในวัฏภาคของเหลว ส่วนการเปรียบเทียบผลของตัวทำละลายอินทรีย์ต่างๆอาทิ เบนซีน เฮปทานอล และ นอร์มัลไพโรลิโดน กับการใช้คาร์บอนไดออกไซด์วิกฤติยิ่งยวดแทนตัวทำละลายในปฏิกิริยาไฮโดรจิเนชันของไซโคลเฮกซีนในวัฏภาคของเหลวพบว่าอัตราการเกิดปฏิกิริยาสูงขึ้นเมื่อใช้คาร์บอนไดออกไซด์วิกฤติยิ่งยวดเนื่องมากจากแก๊สไฮโดรเจนสามารถละลายได้ดีในคาร์บอนไดออกไซด์วิกฤติยิ่งยวดมากกว่าในตัวทำละลายอินทรีย์อย่างไรก็ตามพบการเสื่อมสภาพของตัวเร่งปฏิกิริยาแพลเลเดียมเช่นการซินเทอริงและการถูกชะล้างของโลหะแพลเลเดียมในปริมาณที่ใกล้เคียงกัน

เอกสารแนบ 1

Effect of TiO_2 Crystalline Phase Composition on the Physicochemical and Catalytic Properties of Pd/TiO_2 in Selective Acetylene Hydrogenation

Joongjai Panpranot,* Kunyaluck Kontapakdee, and Piyasan Praserthdam

Center of Excellence on Catalysis and Catalytic Reaction Engineering, Department of Chemical Engineering, Faculty of Engineering, Chulalongkorn University, Bangkok 10330, Thailand

Received: December 20, 2005; In Final Form: February 21, 2006

Pd/TiO_2 catalysts have been prepared using TiO_2 supports consisting of various rutile/anatase crystalline phase compositions. Increasing percentages of rutile phase in the TiO_2 resulted in a decrease in Brunauer−Emmett−Teller surface areas, fewer Ti^{3+} sites, and lower Pd dispersion. While acetylene conversions were found to be merely dependent on Pd dispersion, ethylene selectivity appeared to be strongly affected by the presence of Ti^{3+} in the TiO_2 samples. When TiO_2 samples with 0−44% rutile were used, high ethylene selectivities (58−93%) were obtained whereas ethylene losses occurred for those supported on TiO_2 with 85% or 100% rutile phase. X-ray photoelectron spectroscopy and electron spin resonance experiments revealed that a significant amount of Ti^{3+} existed in the TiO_2 samples composed of 0−44% rutile. The presence of Ti^{3+} in contact with Pd can probably lower the adsorption strength of ethylene resulting in an ethylene gain. Among the five catalysts used in this study, the results for Pd/TiO_2-R44 suggest an optimum anatase/rutile composition of the TiO_2 used to obtain high selectivity of ethylene in selective acetylene hydrogenation.

1. Introduction

Titanium dioxide (TiO_2) is a very useful material and has received great attention in catalysis research as a catalyst, a catalyst support, and a promoter. Due to the strong oxidizing power of its holes, high photostability, and redox selectivity, TiO_2 is one of the most popular and promising catalysts in photocatalytic applications.[1−3] In addition, as a catalyst support particularly in hydrogenation reactions, TiO_2 manifests a strong metal−support interaction (SMSI) with group VIII metals under high reduction temperatures (usually above 300 °C) resulting in an improved catalytic performance.[4,5] For example, Moon et al.[5] reported an improved selectivity for ethylene production in selective acetylene hydrogenation over TiO_2-modified Pd catalysts compared to Pd/SiO_2.

Naturally, TiO_2 has three main crystal structures: anatase, which tends to be more stable at low temperature; brookite, which is usually found in minerals and has an orthorhombic crystal structure, and rutile, which is the stable form at higher temperature.[6] Both rutile and anatase TiO_2 are tetragonal structures with unit cells consisting of 6 and 12 atoms, respectively.[7] Generally, anatase phase TiO_2 shows higher photocatalytic activity than other types of titanium dioxide due to its appropriate band gap energy that corresponds to UV light.[8] Since each crystal structure of TiO_2 possesses different physical properties, the use of TiO_2 with various polymorphs as catalyst supports might exhibit different characteristics and catalytic properties. Nevertheless only a few publications reported the effect of titania polymorph on such differences. Chary et al.[9] reported that MoO_3 dispersed better on anatase TiO_2 than when it was supported on rutile TiO_2. The number of surface Mo sites were directly correlated with the catalytic properties of the catalysts for ammoxidation of 3-picoline to nicotinonitrile. A recent study reveals that the SMSI of Pd/TiO_2 catalysts was also influenced by the titania polymorph.[10] Anatase TiO_2-supported palladium catalyst exhibited SMSI at lower temperatures than a rutile TiO_2-supported one. Jongsomjit et al.[11] have studied cobalt dispersion on TiO_2 and found that the presence of 19% rutile phase in titania facilitates the reduction of highly dispersed cobalt oxide to cobalt metal.

In this study, the physicochemical properties of TiO_2 and Pd dispersed on TiO_2 consisting of various rutile/anatase phase compositions were investigated by means of X-ray diffraction (XRD), N_2 physisorption, scanning electron microscopy (SEM), electron spin resonance (ESR), X-ray photoelectron spectroscopy (XPS), and pulse CO chemisorption methods. Furthermore, the catalytic properties of the Pd/TiO_2 catalysts were evaluated in the gas-phase selective hydrogenation of acetylene in excess ethylene.

2. Experimental Section

2.1. Preparation of TiO_2 and Pd/TiO_2 Catalyst Samples. TiO_2 supports with various rutile/anatase phase compositions were obtained by calcinations of pure anatase titania (Aldrich) in air at temperatures between 900 and 1100 °C for 4 h. The high space velocity of air flow (16 000 h^{-1}) ensured the gradual phase transformation to avoid rapid sintering of the samples. Approximately 1% Pd/TiO_2 was prepared by the incipient wetness impregnation technique using an aqueous solution of the desired amount of $Pd(NO_3)_2$ (Wako). The catalysts were dried overnight at 110 °C and then calcined in N_2 flow 60 cm^3/min with a heating rate of 10 °C/min until the temperature reached 500 °C and then in air flow 100 cm^3/min at 500 °C for 2 h.

2.2. Catalyst Characterization. The Brunauer−Emmett−Teller (BET) surface areas of the samples were determined by N_2 physisorption using a Micromeritics ASAP 2000 automated system. Each sample was degassed under vacuum at <10 μm Hg in the Micromeritics ASAP 2000 at 150 °C for 4 h prior to

* Author to whom correspondence should be addressed. E-mail: joongjai.p@eng.chula.ac.th.

10.1021/jp057395z CCC: $30.25
Published on Web 03/25/2006

N_2 physisorption. The XRD spectra of the catalyst samples were measured from 20° to 80° 2θ using a Siemens D5000 X-ray diffractometer and Cu Kα radiation with a Ni filter. Electron spin resonance spectra were taken at −150 °C using a JEOL JES-RE2X spectrometer. Relative percentages of palladium dispersion were determined by pulsing carbon monoxide over the reduced catalyst. Approximately 0.2 g of catalyst was placed in a quartz tube in a temperature-controlled oven. The amounts of CO chemisorbed on the catalysts were measured using a Micromeritic Chemisorb 2750 automated system attached with ChemiSoft TPx software at room temperature. Prior to chemisorption, the sample was reduced in a H_2 flow at 500 °C for 2 h, then cooled to ambient temperature in a He flow. The particle morphology was obtained using a JEOL JSM-35CF scanning electron microscope operated at 20 kV. The XPS analysis was performed using an AMICUS photoelectron spectrometer equipped with a Mg Kα X-ray as a primary excitation and KRATOS VISION2 software. XPS elemental spectra were acquired with a 0.1 eV energy step at a pass energy of 75 kV. The C 1s line was taken as an internal standard at 285.0 eV. A temperature-programmed desorption (TPD) study was performed in a Micromeritic ChemiSorb 2750 automated system attached with ChemiSoft TPx software. Approximately 0.05 g of a calcined catalyst was placed in a quartz tube in a temperature-controlled oven and connected to a thermal conductivity detector (TCD). The catalyst was first reduced in H_2 flow at 100 cm^3/min for 1 h at 500 °C (using a ramp rate of 10 °C/min) and then cooled to room temperature. The catalyst surface was saturated with ethylene or CO by applying a high purity grade ethylene or CO at 60 mL/min for 3 h. Then the samples were flushed with helium while cooling to room temperature for about 1 h. The temperature-programmed desorption was performed with a constant heating rate of ca. 10 °C/min from 35 to 500 °C. The amount of desorbed ethylene or CO was measured by analyzing the effluent gas with a thermal conductivity detector.

2.3. Reaction Study. Selective acetylene hydrogenation was performed in a quartz tube reactor (i.d. 9 mm). Prior to the start of each run, the catalyst was reduced in H_2 at 500 °C for 2 h. Then the reactor was purged with argon and cooled to the reaction temperature, 40 °C. Feed gas composed of 1.46% C_2H_2, 1.71% H_2, 15.47% C_2H_6, and balanced C_2H_4 (Rayong Olefin Co., Ltd) and a GHSV of 5400 h^{-1} were used. The composition of product and feed stream were analyzed by a Shimadzu GC 8A equipped with a TCD and flame ionization detector (FID) (molecular sieve 5 Å and carbosieve S2 columns, respectively). Acetylene conversion as used herein is defined as moles of acetylene converted with respect to acetylene in feed. Ethylene selectivity is defined as the percentage of acetylene hydrogenated to ethylene over totally hydrogenated acetylene. The ethylene being hydrogenated to ethane (ethylene loss) is the difference between all the hydrogen consumed and all the acetylene that has been totally hydrogenated.

3. Results and Discussion

3.1. Properties of TiO_2 Consisting of Various Rutile/Anatase Phase Compositions. In this study, pure anatase titania was gradually transformed into rutile titania by calcination in air under temperatures ranging between 900 and 1010 °C for 4 h. XRD patterns of the calcined TiO_2 samples are shown in Figure 1. For the pure anatase titania, XRD peaks at 25°, 37°, 48°, 55°, 56°, 62°, 71°, and 75° 2θ were evident. XRD peaks for rutile phase at 28° (major), 36°, 42°, and 57° appeared after calcinations. The amount of rutile phase formed during calcinations depended on the temperature used and was calculated using

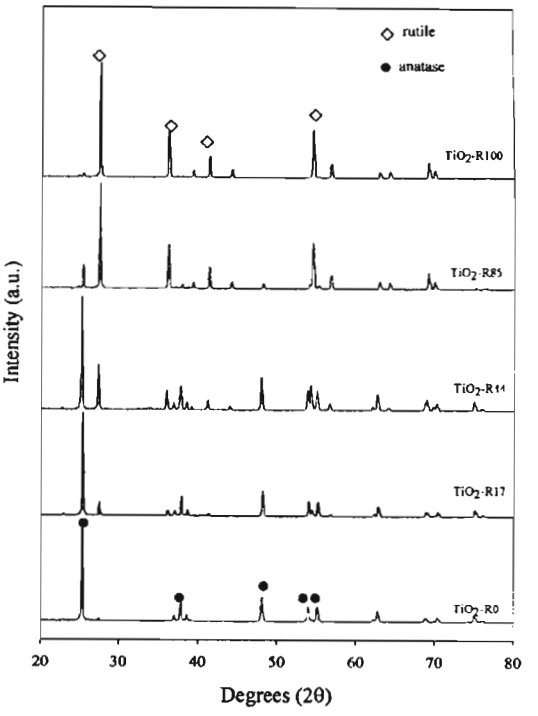

Figure 1. XRD patterns of TiO_2 samples.

the areas of the major anatase and rutile XRD peaks according to the method described by Jung et al.[12] as follows

$$\%\ \text{rutile} = \frac{1}{\left[\left(\frac{A}{R}\right)0.884 + 1\right]} \times 100$$

where A and R are the peak areas for the major anatase (2θ = 25°) and rutile phase (2θ = 28°), respectively.

The titania samples consisting of 0, 17, 44, 85, and 100% rutile phase were named as TiO_2-R0, R17, R44m R85, and R100, respectively. Scanning electron micrographs of various titania samples are shown in Figure 2; agglomeration of the particles is clearly seen with increasing percentage of rutile phase in the TiO_2 samples. After being subjected to the thermal treatment (calcination), BET surface areas of the TiO_2 samples (Table 1) decreased essentially from 64.4 for R0 (pure anatase) to 18.3 m^2/g for R100 (pure rutile). The ESR spectra of the TiO_2 samples are shown in Figure 3. The signals of g values less than 2 were assigned to Ti^{3+} ($3d^1$).[13,14] No Ti^{3+} ESR signal was observed for TiO_2 consisting of ≥85% rutile phase. It is suggested that Ti^{4+} in the TiO_2 with higher percentages of rutile is more difficult to be reduced to Ti^{3+}. As rutile titania is more thermodynamically and structurally stable than anatase titania, the Ti^{3+} ions fixed in the surface lattice of anatase TiO_2 are easier to diffuse to the surface those in the surface lattice of rutile TiO_2.[10] The results in this study suggest a threshold limit of maximum percentage of rutile in the TiO_2 sample so that the presence of Ti^{3+} can be detected by the ESR technique.

The survey XPS spectra for pure rutile and anatase TiO_2 samples were recorded with a photon energy of 1256 eV (Mg Kα), the kinetic energies of the emitted electrons being in the range of 0−1000 eV. The core level XPS spectra of Ti 2p recorded from various TiO_2 samples (results not shown) show sharp and intense peaks at binding energies 464.2 and 458.5 eV, indicating of only Ti^{4+} in the TiO_2.[15,16] No Ti^{3+} XPS spectra

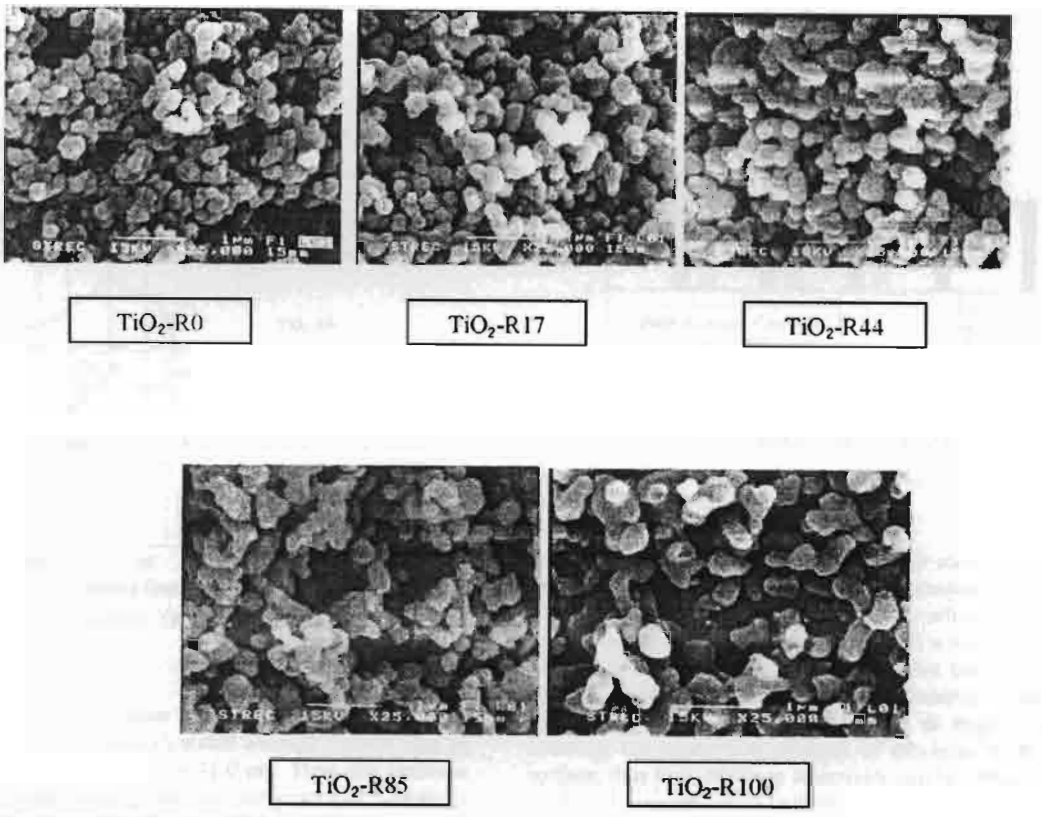

Figure 2. SEM micrographs of various TiO_2 samples.

TABLE 1: TiO_2 Samples Consisting of Various % Rutile

sample	% rutile	BET surface area (m^2 g)
TiO_2-R0	0	64.4
TiO_2-R17	17	38.6
TiO_2-R44	44	25.0
TiO_2-R85	85	23.5
TiO_2-R100	100	18.3

were seen for all the TiO_2 samples under these conditions. It is likely that there was an oxygen-rich layer near the surface of the TiO_2 particles, which is formed by oxygen adsorption and easy oxidation of the titanium surface.[17] To observe the reduced Ti species (i.e., Ti^{3+}, Ti^{2+}) that might exist in the bulk of the TiO_2 samples, TiO_2 surfaces were subjected to an argon-ion bombardment for 2 min. Ti 2p XPS spectra of the Ar^+-etched TiO_2 samples are illustrated in Figure 4. The presence of new Ti $2p^{1/2}$ and $2p^{3/2}$ peaks at lower binding energies of 461.2 and 456.5 eV indicated Ti^{3+} species in the TiO_2.[15,16,18,19] It was found that the intensities of Ti^{3+} for both Ti $2p^{1/2}$ and $2p^{3/2}$ peaks increased with decreasing percentages of the rutile phase. The results were found to be in accordance with our ESR results. Moreover, Ti 2p peaks indicative of Ti^{2+} species[17,19] were also observed at binding energies of 451.8 and 454.3 eV for TiO_2 samples with low percentages of the rutile phase.

3.2. Dispersion of Pd on the TiO_2 Surface. Dispersion of the active surface Pd on TiO_2 consisting of various rutile-anatase phase compositions was investigated by means of CO pulse chemisorption and XPS techniques, and the results are given in Table 2. Since palladium hydride can be formed in the presence of hydrogen, CO chemisorption is typically preferred rather than H_2 chemisorption for the measurement of active palladium surface with the assumption that one carbon monoxide

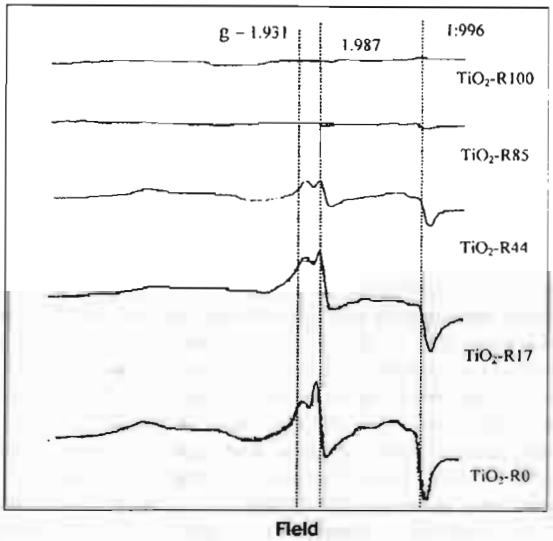

Figure 3. ESR spectra of TiO_2 samples.

molecule adsorbs on the palladium site.[20-25] The BET surface areas of the TiO_2-supported Pd catalysts were slightly less than that of the original TiO_2 supports suggesting that palladium was deposited in some of the pores of TiO_2. It would appear that the particle size and shape of the catalyst particles were not affected by impregnation of palladium (no changes in the particle size shape). Since no XRD peaks of PdO or Pd^0 were observed for the catalyst samples after calcinations at 450 °C for 3 h, it suggests that palladium was highly dispersed on the titania surface (results not shown). It was found that as the percentage of the rutile phase increased from 0 to 100% the amount of CO

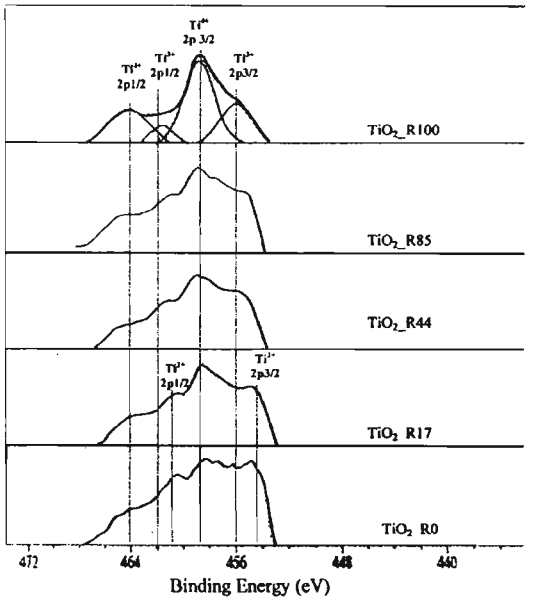

Figure 4. XPS Ti 2p spectra of TiO_2 samples after 2 min of etching by Ar^+.

chemisorption decreased from 2.23×10^{18} to 1.55×10^{18} molecules of CO while the calculated average particle size of Pd^0 metal increased from 28.5 to 41.0 nm. Thus, the presence of rutile phase significantly decreased dispersion of palladium on the titania supports. XPS analysis revealed an increasing Pd surface concentration with increasing percentages of rutile up to ca. 44% rutile. Further increases in the percentage of the rutile phase did not result in a higher concentration of Pd on the TiO_2 surface and could lower the Pd surface concentration for pure rutile TiO_2.

3.3. Selective Acetylene Hydrogenation on Pd/TiO_2 Catalysts. To investigate the catalytic performance of Pd/TiO_2 catalysts consisting of various rutile phase percentages, selective hydrogenation of acetylene to ethylene was performed in a fixed bed flow reactor. Removal of a trace amount of acetylene in an ethylene feed stream is vital for the commercial production of polyethylene since acetylene acts as a poison to the polymerization catalysts. Figure 5 shows acetylene conversions and ethylene selectivities obtained from various Pd/TiO_2 catalysts. Acetylene conversions were in the range of 40−59% and were found to be merely dependent on the Pd dispersion. However, a rapid change of catalytic properties in terms of ethylene selectivity was observed. When the TiO_2 supports with rutile contents of 44% or less were employed, ethylene selectivities were positive varied from 58 to 93% with a maximum for the Pd/TiO_2-R44. On the contrary, ethylene selectivities became negative when Pd catalysts supported on TiO_2 consisting ≥85% rutile phase were used resulting in ethylene losses. Overhydrogenation of ethylene to ethane was likely to occur for such cases. Ethylene hydrogenation is usually believed to take place on the

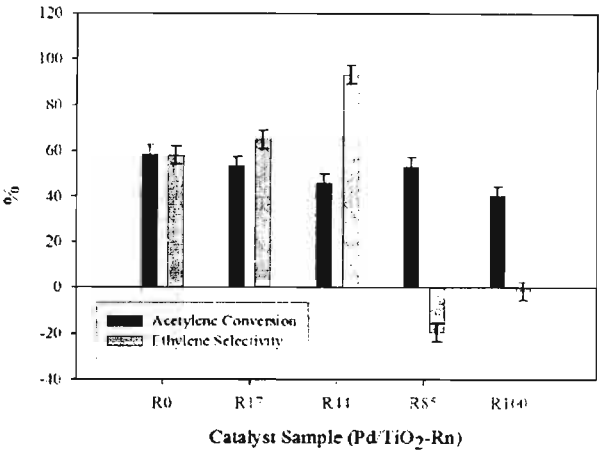

Figure 5. Catalytic performances of various Pd/TiO_2 catalysts in selective acetylene hydrogenation.

support by means of a hydrogen transfer mechanism.[26] There may be some relationship between the presence of Ti^{3+} ions in the TiO_2 supports and the high ethylene selectivity since only the Pd catalysts supported on TiO_2 with a significant amount of Ti^{3+} yielded high ethylene gains. This could probably be explained in terms of the SMSI effect. Generally, SMSI occurs for Pd/TiO_2 catalysts after reduction at high temperature, lowering the adsorption strength of ethylene on the catalyst surface; thus high ethylene selectivity can be obtained.[5] In this work, the amounts of CO adsorbed on the catalysts reduced at 500 °C were much smaller than those reduced at room temperature. Since the CO adsorption ability of the catalysts can be recovered (restored) so that the decline in the amount of CO adsorbed at high-temperature reduction was caused by an SMSI effect and not by metal sintering. Detailed experimental observation of the reversibility of the SMSI effect for group VIII metals in oxidizing atmospheres can be found in ref 27. It is also known that suppression of H_2 chemisorption occurs on such catalysts similar to that of CO. Recently, Fan et al. suggested that diffusion of Ti^{3+} from the lattice of anatase TiO_2 to surface Pd particles can lower the temperature to induce SMSI.[10]

The characteristics of the surface active sites of the catalysts were studied by means of the temperature-programmed desorption of CO and ethylene from 50 to 500 °C. The results are shown in Figures 6A and 6B, respectively. Similar profiles were found for both CO and ethylene temperature-programmed desorption in which two main desorption peaks were observed. Such results suggest that there were two different active sites on the catalysts, probably Pd and Ti^{3+} sites. Since the high-temperature peaks were diminished with increasing percentages of rutile in the TiO_2 supports, these peaks could be attributed to the adsorption on Ti^{3+} sites. The low-temperature peaks, therefore, were attributed to adsorption on Pd sites. Adsorption of CO on Ti^{3+} sites has also been observed by an IR study by Benvenutti et al.[28]

TABLE 2: Physicochemical Properties of Pd/TiO_2 Catalysts

sample	BET surface area (m^2/g)	CO chemisorption × 10^{18} (molecule CO/g catalyst)	Pd dispersion (%)	d_p Pd^0 (nm)	atomic concentration Pd/Ti
Pd/TiO_2-R0	44.5	2.23	3.93	28.5	0.084
Pd/TiO_2-R17	27.1	2.20	3.87	28.9	0.116
Pd/TiO_2-R44	20.1	1.66	2.92	38.3	0.196
Pd/TiO_2-R85	19.8	1.77	3.12	35.9	0.199
Pd/TiO_2-R100	17.2	1.55	2.73	41.0	0.168

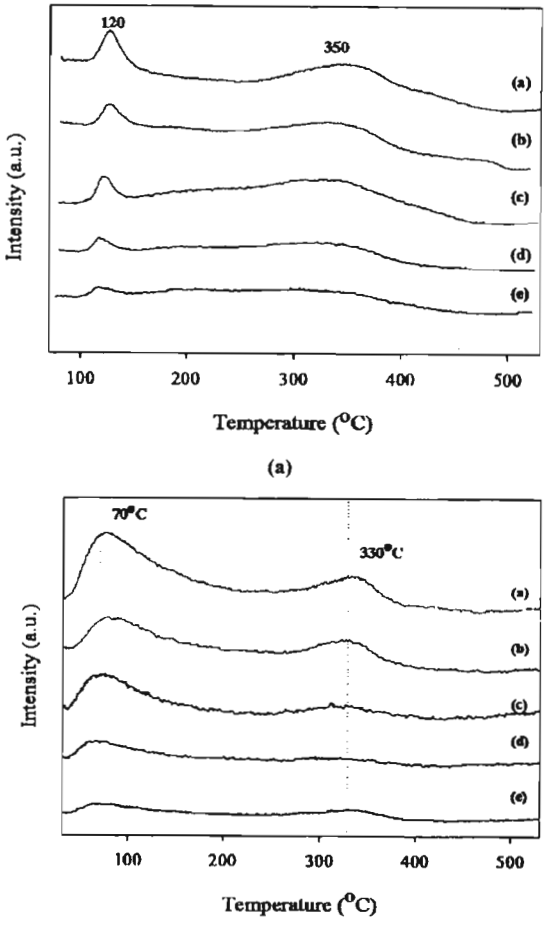

Figure 6. Temperature-programmed desorption of (A) CO and (B) C_2H_4 for the various Pd/TiO_2 catalysts: (a) Pd/TiO_2-R0, (b) Pd/TiO_2-R17, (c) Pd/TiO_2-R44, (d) Pd/TiO_2-R85, (e) Pd/TiO_2-R100.

In our study, we propose that ethylene can adsorb on Ti^{3+} sites and hydrogenate to ethane. However, simultaneously Ti^{3+} species that were in contact with the palladium surface promoted the SMSI effect and ethylene desorption.[10] Thus, without Ti^{3+} on the TiO_2 surface, low selectivity for ethylene was observed (as seen for the cases of Pd/TiO_2-R85 and Pd/TiO_2-R100) while with too many Ti^{3+} (that were not in contact with Pd) ethylene hydrogenation also occurred. Therefore, among the three catalysts with significant amounts of Ti^{3+} used in this study, Pd/TiO_2-R44 exhibited higher ethylene gains than Pd/TiO_2-R17 and Pd/TiO_2-R0, respectively. The proposed mechanism for acetylene hydrogenation on different types of active sites on Pd/TiO_2 catalysts is illustrated in a conceptual model in Figure 7. In a previous study from our group, two types of solvothermal-derived pure anatase TiO_2-supported Pd catalysts were prepared and studied in acetylene hydrogenation. It was found that the one containing a higher amount of Ti^{3+} exhibited slightly lower ethylene selectivity.[29] The results from the present study, however, emphasize the influence of Ti^{3+} present in the TiO_2 samples on their catalytic behavior; the results for Pd/TiO_2-R44 suggest the best (optimum) anatase/rutile composition of the TiO_2 used to obtain high selectivity of ethylene in selective acetylene hydrogenation.

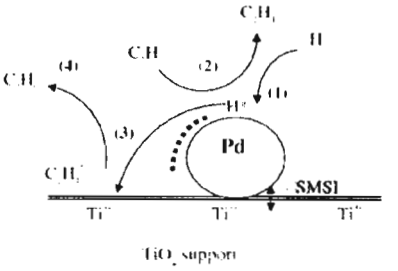

Figure 7. Conceptual model for selective acetylene hydrogenation mechanism on Pd/TiO_2 catalysts: (1) H_2 transfer from the metal to the support, (2) acetylene hydrogenation to ethylene followed by ethylene desorption, (3) adsorption of ethylene on Ti^{3+} sites, (4) hydrogenation of ethylene to ethane

4. Conclusions

The physicochemical and catalytic properties of Pd/TiO_2 catalysts can be significantly influenced by the anatase/rutile crystalline phase composition of the TiO_2 supports. Higher percentages of rutile in TiO_2 resulted in a decrease in BET surface areas and fewer Ti^{3+} sites. The presence of Ti^{3+} in the Pd/TiO_2 catalysts appeared to promote ethylene selectivity in selective acetylene hydrogenation when Ti^{3+} sites were in contact with Pd. Among the five crystalline phase compositions of titania used in this study, the one containing 44% rutile was found to be the best (optimum) composition to prepare TiO_2-supported Pd catalysts with high ethylene selectivity.

Acknowledgment. Financial support from the Thailand Research Fund, Rayong Olefins Co., Ltd., and the Graduate School of Chulalongkorn University is gratefully acknowledged.

References and Notes

(1) Ohtani, B.; Ogawa, Y.; Nishimoto, S. *J. Phys. Chem. B* **1997**, *101*, 3746.
(2) Stafford, U.; Gray, K. A.; Kamat, P. V. *J. Catal.* **1997**, *167*, 25.
(3) Herrmann, J.-M. *Catal. Today* **1999**, *53*, 115.
(4) Tauster, S. J.; Fung, S. C.; Garten, R. L. *J. Am. Chem. Soc.* **1978**, *100*, 170.
(5) Kang, J. H.; Shin, E. W.; Kim, W. J.; Park, J. D.; Moon S. H. *J. Catal.* **2002**, *208*, 310.
(6) Rao, C. N. R.; Yuganarasimhan, S. R.; Faeth, P. A. *Trans. Faraday Soc.* **1961**, *57*, 504.
(7) Stashans, A.; Lunell, S.; Grimes, R. W. *J. Phys. Chem. Solids* **1996**, *57*, 1293.
(8) Yin, H.; Wada, Y.; Kitamura, T.; Kambe, S.; Murasawa, S.; Mori, H.; Sakata, T.; Yanagida S. *J. Mater. Chem.* **2001**, *11*, 2694.
(9) Chari, K. V. R.; Bhaskar, T.; Seela, K. K.; Lakshmi, K. S.; Reddy, K. R. *Appl. Catal., A* **2001**, *208*, 291.
(10) Li, Y.; Xu, B.; Fan, Y.; Feng, N.; Qiu, A.; Miao, J.; He, J.; Yang, H.; Chen, Y. *J. Mol. Catal. A: Chem.* **2004**, *216*, 107.
(11) Jongsomjit, B.; Wongsalee, T.; Praserthdam, P. *Mater. Chem. Phys.* **2005**, *92*, 572.
(12) Jung, K. Y.; Park, S. B. *J. Photochem. Photobiol., A* **1999**, *127*, 117.
(13) Conesa, J. C.; Malet, P.; Unuera, G. M.; Sanz, J.; Soria, J. *J. Phys. Chem.* **1984**, *88*, 2986.
(14) Salama, T. M.; Hattori, H.; Kita, H.; Ebitani, K.; Tanaka, T. *J. Chem. Soc., Faraday Trans.* **1993**, *89* (12), 2067.
(15) Liqiang, J.; Xiaojun, S.; Weimin, C.; Zili, X.; Yaoguo, D.; Honggang, F. *J. Phys. Chem. Solids* **2003**, *64*, 615.
(16) Price, N. J.; Reifz, J. B.; Madix R. J.; Solomon, E. I. *J. Electron Spectrosc. Relat. Phenom.* **1999**, *98*−*99*, 257.
(17) Zhang, F.; Zheng, Z.; Liu, D.; Mao, Y.; Chen, Y.; Zhou, Z.; Yang, S.; Liu, X. *Nucl. Instrum. Methods Phys. Res., Sect. B* **1997**, *132*, 620.
(18) Kumar, P. M.; Badrinarayanan, S.; Sastry, M. *Thin Solid Films* **2000**, *358*, 122.
(19) Charles, E.; Sykes, H.; Tikhov, M. S.; Lambert, R. M. *J. Phys. Chem. B* **2002**, *106*, 7290.
(20) Mahata, N.; Vishwanathan, V. *J. Catal.* **2000**, *196*, 262.

(21) Ali, S. H.; Goodwin, J. G., Jr. *J. Catal.* **1998**, *176*, 3.
(22) Sales, E. A.; Bugli, G.; Ensuque, A.; Mendes, M. J.; Bozon-Verduraz, F.; *Phys. Chem. Chem. Phys.* **1999**, *1*, 491.
(23) Sarkany, A.; Zsoldos, Z.; Furlong, B.; Hightower, J. W.; Guczi, L. *J. Catal.* **1993**, *141*, 566.
(24) Vannice, M. A.; Wang, S. Y.; Moon, S. H. *J. Catal.* **1981**, *71*, 152.
(25) Nag, N. K. *Catal. Lett.* **1994**, *24*, 37.
(26) Aplund, S. *J. Catal.* **1996**, *158*, 267.
(27) Stevenson, S. A.; Dumesic, J. A.; Baker, R. T. K.; Ruckenstein, E. *Metal−Support Interactions in Catalysis, Sintering, and Redispersion*; Van Nostrand Reinhold: New York, 1987.
(28) Benvenutti, E. V.; Franke, L.; Moro, C. C. *Langmuir* **1999**, *15*, 3140.
(29) Panpranot, J.; Nakkararuang, L.; Ngamsom, B.; Praserthdam, P. *Catal. Lett.* **2005**, *103*, 53.

เอกสารแนบ 2

Available online at www.sciencedirect.com
SCIENCE DIRECT
ELSEVIER
Journal of Molecular Catalysis A: Chemical 253 (2006) 20–24
JOURNAL OF MOLECULAR CATALYSIS A: CHEMICAL
www.elsevier.com/locate/molcata

A comparative study of liquid-phase hydrogenation on Pd/SiO_2 in organic solvents and under pressurized carbon dioxide: Activity change and metal leaching/sintering

Joongjai Panpranot[a,*], Kunnika Phandinthong[a], Piyasan Praserthdam[a], Masashi Hasegawa[b], Shin-ichiro Fujita[b], Masahiko Arai[b]

[a] *Center of Excellence on Catalysis and Catalytic Reaction Engineering, Department of Chemical Engineering, Faculty of Engineering Chulalongkorn University, Bangkok, Thailand*
[b] *Division of Chemical Process Engineering, Graduate School of Engineering, Hokkaido University, Sapporo, Japan*

Received 7 February 2006; received in revised form 1 March 2006; accepted 1 March 2006

Abstract

Liquid-phase hydrogenation of cyclohexene under mild conditions on Pd/SiO_2 in different organic solvents (benzene, heptanol, and NMP), under pressurized carbon dioxide, and under solvent less condition were investigated and compared. In the cases of using organic solvents, the hydrogenation rates depended on polarity of the solvents in which the reaction rates in high polar solvents such as heptanol and NMP were lower than that in a non-polar solvent. Hydrogenation rates were much higher when the reactions were performed under high-pressure CO_2 or under solvent less condition. The use of high-pressure CO_2 can probably enhance H_2 solubility in the substrate resulting in a higher hydrogenation activity. However, metal sintering and leaching in the presence of high-pressure CO_2 were comparable to those in organic solvents.

Keywords: Liquid phase hydrogenation; Cyclohexene; Pd/SiO_2; Leaching; Sintering; High-pressure CO_2

1. Introduction

Catalytic hydrogenation is one of the most useful, versatile, and environmentally acceptable reaction routes available for organic synthesis, and the reaction is usually carried out in a liquid-phase using batch type slurry processes and a supported noble metal (Pd, Pt, or Rh) catalyst [1–4]. The major advantages of multi-phase catalytic reactions using solid catalysts include easy separation of catalysts and products, easy recovery and catalyst recycling, and relatively mild operating conditions [5,6]. The performance of noble metal catalysts in liquid-phase hydrogenation has been found to be dependent on several factors such as liquid composition (substrate structure, solvent effect, etc.), catalyst nature (active sites composition and morphology, support effect, modifiers, etc.), and reaction conditions (temperature, pressure, etc.) [7]. Deactivation of metal catalysts in liquid-phase reactions can occur even under mild reaction conditions because of sintering and/or leaching of active components, poisoning of active sites by heteroatom-containing molecules, inactive metal or metal oxide deposition, impurities in solvents and reagents, and oligomeric or polymeric by-products. The mechanisms for such deactivation causes, however, have not been fully understood.

Supercritical fluids particularly carbon dioxide (CO_2) as an environmentally benign reaction media offer many advantages compared to conventional organic solvents because they facilitate heat and mass transfer in the reactor and enable easy separation of the solvents from the reactants and products [8–10]. Despite numerous studies in the literature on the successful application of supercritical solvents in catalytic reactions [11–17], the performance of the catalyst in terms of both activity and deactivation in supercritical solvents has not often been compared to those performed in conventional organic solvents. Baiker and co-workers [18] showed that the rate of citral hydrogenation in carbon dioxide under single-phase conditions was about two orders of magnitude higher than in organic solvent. For

* Corresponding author. Tel.: +66 2 2186 869; fax: +66 2 2186 877.
E-mail address: joongjai.p@eng.chula.ac.th (J. Panpranot).

1381-1169/$ – see front matter © 2006 Elsevier B.V. All rights reserved.
doi:10.1016/j.molcata.2006.03.001

hydrogenation of nitrobenzene in supercritical CO_2 on Pt/C catalysts, selectivity to aniline was twice as high as that in ethanol at a similar conversion [19]. It is not clear, however, whether deactivation of supported noble metal catalyst occurred to a similar degree in high-pressure carbon dioxide compared to those in organic solvents.

In this study, we have made a comparative study of catalytic activity and metal leaching/sintering of Pd/SiO_2 catalysts during liquid-phase hydrogenation in different organic solvents, under pressurized carbon dioxide, and under solvent less condition. The metal leaching and sintering are a major cause for catalyst deactivation, which have been investigated by means of X-ray diffraction, atomic absorption spectroscopy, and CO pulse chemisorption method. Liquid-phase hydrogenation of cyclohexene under mild conditions at 0.1 MPa H_2 pressure was used as a test reaction where the rate of reaction can be studied easily.

2. Experimental

2.1. Catalyst preparation and nomenclature

Pd/SiO_2 whose Pd loading was approximately 1 wt.% was prepared by ion-exchange using $Pd(NH_3)_4Cl_2$ (Aldrich) and a silica gel (Aldrich, Davisil grade 646). A 20 mmol/l palladium solution was prepared by using 0.152 g of $Pd(NH_3)_4Cl_2$ and a certain amount of distilled water. Then 5.0 cm^3 of the palladium solution was diluted with distilled water to 30 ml. Approximately 1.0 g of silica gel was immersed into the solution and the pH value was adjusted to 12 by adding 25% NH_4OH solution. The support was kept immersed in this solution at room temperature for 3 days. After filtration, the solid residue was washed with distilled water until pH 7.0 and vacuum dried over night at room temperature. The catalysts were calcined in air at 450 °C for 3 h and were denoted as "fresh catalyst" in this work. Prior to the hydrogenation reaction, the catalyst was reduced in H_2 at 25 °C for 2 h. After the reaction runs, the catalysts were re-calcined in air at 450 °C for 3 h in order to remove any carbon deposit and were denoted as "spent catalysts".

2.2. Catalyst characterization

The bulk composition of palladium was determined using a Varian Spectra A800 atomic absorption spectrometer. The X-ray diffraction patterns of the catalysts were measured in a range of 2θ value between 20° and 80° using a SIEMENS D5000 X-ray diffractometer and Cu Kα radiation with a Ni filter. The number of surface palladium atoms was determined from CO chemisorption by a pulse method and the palladium dispersion was estimated from the amount of CO chemisorbed assuming a stoichiometry of CO/palladium = 1. Approximately 0.2 g of catalyst was placed in a quartz tube in a temperature-controlled oven and reduced in a flow of hydrogen (50 cm^3/min) at room temperature for 2 h. Then, the sample was purged at this temperature with helium for 1 h. Carbon monoxide was pulsed at room temperature over the reduced catalyst until the TCD signal from a pulse (at the exit) became constant.

2.3. Reaction study

Liquid-phase hydrogenation in conventional organic solvents was carried out in a 100 cm^3 stainless steel autoclave. The Pd/SiO_2 catalyst of 0.2 g was placed in the reactor with 20 mmol of cyclohexene (Aldrich) and 48 cm^3 of solvents. For the reaction runs under high-pressure CO_2 and under solvent less condition, a 50 cm^3 stainless steel autoclave was used in order to compare the reaction with a similar substrate/solvent ratio. For the application of high-pressure CO_2, the reactor was purged with CO_2 and then hydrogen was introduced to the desired pressure, followed by introduction of CO_2 to the desired pressure using a high-pressure liquid pump. Stirring was switched on to start the reaction. The products were analyzed by GC and GC–MS. Phase behavior during reaction in high-pressure CO_2 was inspected using a 10 cm^3 high-pressure sapphire-windowed view cell.

3. Result and discussion

3.1. Liquid-phase hydrogenation in different solvents

Catalyst activities for liquid-phase hydrogenation of cyclohexene at 25 °C in various organic solvents, under pressurized carbon dioxide, and under solvent less condition are shown in Table 1. It is obvious that the hydrogenation rates are much higher for those performed in high-pressure CO_2 than those carried out in organic solvents. In hydrogenation reaction, H_2 solubility in common organic solvents is usually low depending on the nature of the solvent. It has been reported that hydrogenation activity decreases with increasing solvent polarity due to competitive adsorption of high polar solvent and substrate on the catalyst surface [20,21]. Similar trend was observed in this study; as the polarity of the solvent increases in the order of NMP > heptanol > benzene, the hydrogenation activity decreases in the order NMP < heptanol < benzene. Since the concentration of either cyclohexene or H_2 in high-pressure CO_2 was different from those in organic solvents, it is not easy to compare the results at 6 MPa CO_2 with those in organic solvents. However, compared to that under the solvent less condition, the hydrogenation rate increases from 93% to nearly 100% in the presence of high-pressure CO_2. A gas–liquid-phase boundary

Table 1
Catalytic activities of Pd/SiO_2 for cyclohexene hydrogenation[a] in various solvents

Solvent	Polarity	Time (min)	Conversion (%)
NMP	4.09	10	15.1
Heptanol	1.33	10	27.6
Benzene	0.0	10	57.0
Cyclohexene	0.0	2	93.0
		10	96.0
CO_2 6 MPa	0.0	2	~100.0
		10	~100.0

Dipole moment (debye) [26]. Under solvent-less conditions. Liquid (substrate)-gas two phases (except for a solid phase of catalyst).

[a] Reaction conditions: T = 25 °C, H_2 = 1 MPa, catalyst/substrate = 0.1 g cat./10 mmol substrate, and substrate/solvent = 1/24 (v/v).

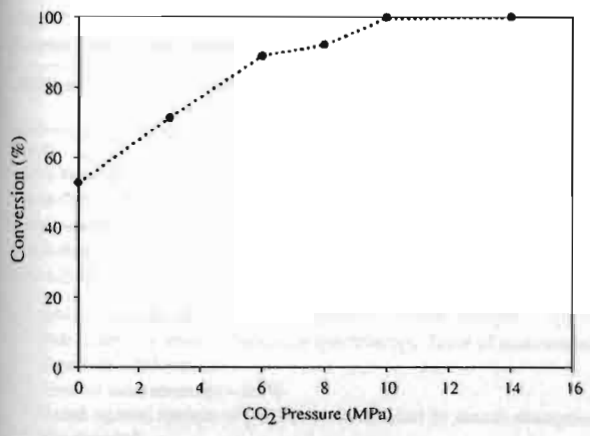

Fig. 1. Effect of CO_2 pressure on the hydrogenation activities of Pd/SiO_2 (the reaction conditions were $T = 40\,^{\circ}C$, $H_2 = 5$ MPa, 0.005 g cat., 20 mmol cyclohexene, and reaction time 3 min).

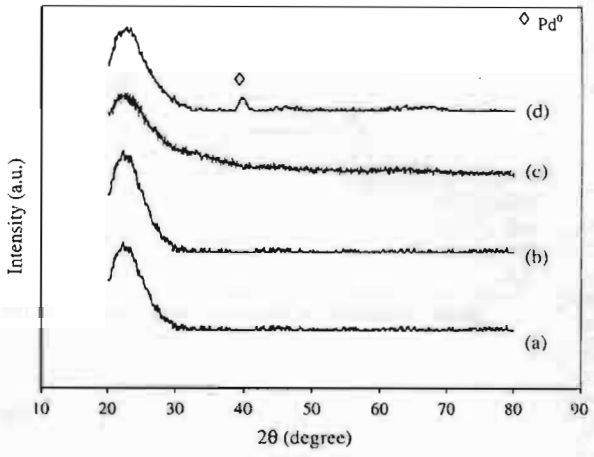

Fig. 2. XRD patterns of Pd/SiO_2 catalysts: (a) after first calcination and (b) after reduced in H_2 at room temperature; (c) after reduced and re-calcination (without reaction) and (d) after reduced and reaction in NMP.

was still observed from visual observations under the reaction conditions used, and so the hydrogenation occurs mainly in the nearly pure substrate liquid phase. The H_2 concentration in the liquid phase may be enhanced by dissolution of CO_2, resulting in the increase of the hydrogenation rate at high CO_2 pressure.

The effect of CO_2 pressure on liquid-phase hydrogenation of cyclohexene on Pd/SiO_2 catalysts was investigated for CO_2 pressure in the range between 0 and 14 MPa at 40 °C where CO_2 can be in the supercritical state. The results are shown in Fig. 1. It is seen that the hydrogenation rate increases with increasing CO_2 pressure. Phase behavior study revealed that the mixture of cyclohexene and CO_2 (without catalyst) was gas–liquid two phases at pressures up to 9 MPa but a single phase at 9.4 MPa or above. Nearly 100% cyclohexene conversions were observed under those homogeneous conditions. Arai and co-workers [22] has recently suggested that hydrogenation rate in dense carbon dioxide strongly correlates with the phase behavior of the reaction mixture. In selective hydrogenation of cinnamaldehyde using ruthenium–phosphine complex catalysts, total conversion and cinnamyl alcohol increased with increasing CO_2 pressure when the reactions were carried out in an organic solvent free two-phase system.

3.2. Metal sintering and leaching during hydrogenation

Under the reaction conditions studied, metal leaching and metal sintering were observed and for some cases were found to be in large extents. The XRD patterns of the fresh catalysts (after first calcination), after reduction in H_2 at room temperature, after reduction and re-calcination (without reaction), and after reduction and being used in hydrogenation reaction with NMP solvent are shown in Fig. 2. There was no significant change in the XRD patterns of the calcined, the reduced, and the re-calcined catalysts (without reaction) since only a broad peak for SiO_2 is observed at $2\theta = 22°$. XRD characteristic peaks for palladium oxide (PdO) or metallic Pd^0 are not detected, suggesting that palladium is highly dispersed on the silica support and its crystallite size is smaller than the XRD detectable limit. However, XRD characteristic peak for metallic Pd^0 was observed after reduced and being used in hydrogenation reaction. Therefore, metal sintering did not occur by the reduction at ambient temperature or by thermal effects during the calcination at 450 °C. After being subjected to the hydrogenation reaction runs, the catalysts were re-calcined at 450 °C for 3 h in order to remove any carbon deposits. The XRD patterns of these so-called spent catalysts are shown in Fig. 3. The diffraction peaks for PdO are now evident at $2\theta = 33.8°$, 42.0°, 54.8°, 60.7° and 71.4° for all the spent catalysts, showing that the metal sintering occurred during the liquid-phase hydrogenation reaction, since no XRD peak of PdO was detected over the re-calcined catalyst (Fig. 2). The PdO crystallite sizes were calculated from the full width at half maximum of the XRD peak at $2\theta = 33.8°$ using Scherrer equation and are reported in Table 2. The crystallite sizes of PdO on the spent catalysts are in the order of solvent-less < benzene < CO_2 < heptanol < NMP.

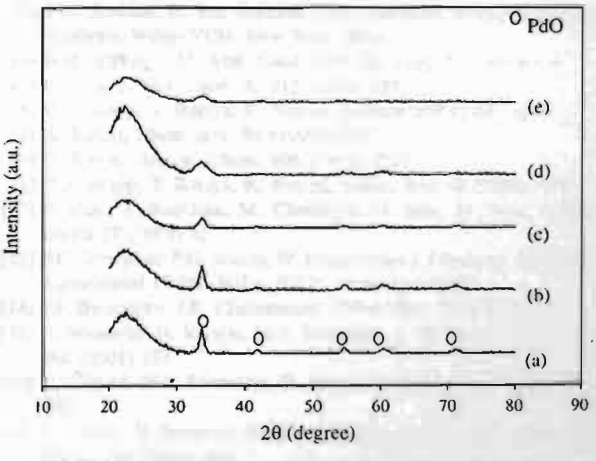

Fig. 3. XRD patterns of re-calcined spent Pd/SiO_2 catalysts after hydrogenation reaction in various solvents: (a) NMP, (b) heptanol, (c) CO_2 6 MPa, (d) solvent less and (e) benzene.

Table 2
Characteristic of fresh and spent[a] Pd/SiO_2 catalysts

Catalyst	PdO particle size[c] (nm)	Amount of Pd[b] (wt.%)	Pd leached (%)	Amount of CO chemisorbed[d] $\times 10^{19}$ (molecule/g cat.)	Pd dispersion[e] (%)
Fresh	n.d.[f]	0.97	–	2.43	44.3
Spent-benzene	3.9	0.86	11.3	1.00	20.6
Spent-CO_2 6 MPa	7.6	0.77	20.6	0.61	14.0
Spent-solvent less	3.5	0.85	12.4	0.38	6.9
Spent-heptanol	10.3	0.82	15.5	0.18	3.9
Spent-NMP	11.0	0.76	21.6	0.16	3.8

[a] Reaction conditions: T, 25 °C; H_2 pressure, 1 MPa; catalyst, 0.1 g; substrate, 10 mmol; substrate/solvent, 1/24 (v/v), reaction time = 10 min.
[b] Determined by atomic absorption spectroscopy. Error of measurements = ±5%.
[c] Based on XRD results.
[d] Error of measurements = ±5%.
[e] Based on total amount of palladium determined by atomic absorption spectroscopy.
[f] Not detected.

The actual amounts of palladium loading determined by atomic absorption spectroscopy and the CO chemisorption results for all the catalysts are also given in Table 2. The palladium loading on the fresh catalyst is 0.97 wt.% and those on the spent catalysts are always lower than that on the fresh catalyst, meaning that palladium was leached in the course of the reaction. Leaching of active metal is another main cause of catalyst deactivation in liquid-phase reaction. In general, it depends upon the reaction medium (pH, oxidation potential, chelating properties of molecules) and upon bulk and surface properties of the metal [23]. In this study, the percentages of the leaching are between 11 and 22% and there is no correlation between the amount of metal leached and the polarity of solvent employed (see Table 1). The amount of CO chemisorbed, i.e. the number of surface Pd atoms, significantly decreased by 60% or more for all the spent catalysts. The decreases in the amount of CO adsorbed are much more than those expected from the results for the Pd leaching. This would be caused by the Pd sintering. The Pd dispersions determined for the spent catalysts are below 50% of for the fresh catalyst. The extent of the Pd sintering depends on the solvent employed for the reaction and is significant in heptanol and NMP. The Pd dispersions of the spent catalysts used in these polar solvents are below 10% of that of the fresh catalyst.

Sintering of supported metal particles in liquid-phase reactions is typically irreversible and can occur even at ambient temperature because of atomic migration processes involving the extraction and transport of surface metal atoms by chelating molecules [23]. The use of high polar solvents such as NMP and heptanol appeared to promote such processes. Some of the leached metal species probably re-deposited on surfaces of the support and/or the Pd particles remaining on the catalysts, causing the sintering as suggested earlier by Arai and co-workers for sintering of Pd/C during Heck coupling reaction [24,25].

4. Conclusions

The study provides a cautionary note for selection of a solvent used in liquid-phase hydrogenation. The use of high polar organic solvents can result in low hydrogenation activities as well as significant metal sintering and metal leaching during reaction. Compared to the use of organic solvents or solvent less, the use of high-pressure CO_2 enhanced the hydrogenation activity of Pd/SiO_2 catalyst. However, metal sintering and leaching in the presence of high-pressure CO_2 were comparable to those in organic solvents.

Acknowledgements

The financial supports of the Thailand Research Fund (TRF), TJTTP-JBIC, and the Graduate School of Chulalongkorn University are gratefully acknowledged. The authors also would like to thank Fengyu Zhao and Jianmin Sun for their supports.

References

[1] P.N. Rylander, Hydrogenation Methods, Academic Press, New York, 1985.
[2] L. Guczi, A. Horvath, A. Beck, A. Sarkany, Stud. Surf. Sci. Catal. 145 (2003) 351.
[3] O. Dominguez-Quintero, S. Martinez, Y. Henriquez, L. D'Ornelas, H. Krentzien, J. Osuna, J. Mol. Catal. A 197 (2003) 185.
[4] K.J. Stanger, Y. Tang, J. Anderegg, R.J. Angelici, J. Mol. Catal. A. 202 (2003) 147.
[5] R.A. Sheldon, H. Van Bekkum, Fine Chemicals through Heterogeneous Catalysis, Wiley–VCH, New York, 2001.
[6] B.M. Bhanage, M. Arai, Catal. Rev. Sci. Eng. 43 (2001) 315.
[7] P. Nitta, J. Mol. Catal. A. 212 (2004) 155.
[8] P.G. Jessop, T. Ikariya, R. Noyori, Science 269 (1995) 1065.
[9] A. Baiker, Chem. Rev. 99 (1999) 453.
[10] G. Kaupp, Angew. Chem. 106 (1994) 1519.
[11] P.G. Jessop, T. Ikariya, R. Noyori, Chem. Rev. 99 (1999) 475.
[12] F. Zhao, I. Ikushima, M. Chatterjee, O. Sato, M. Arai, J. Supercrit. Fluids 27 (2003) 65.
[13] P.G. Jessop, in: P.G. Jessop, W. Leitner (Eds.), Chemical Synthesis Using Supercritical Fluids, Wiley–VCH, Weinheim, 1999.
[14] J.F. Brennecke, J.E. Chateauneuf, Chem. Rev. 99 (1999) 433.
[15] R. Wandeler, N. Kunzle, M.S. Schneider, T. Mallat, A. Baiker, J. Catal. 200 (2001) 377.
[16] L. Schmid, M.S. Schneider, D. Engel, A. Baiker, Catal. Lett. 88 (2003) 105.
[17] F.Y. Zhao, Y. Ikushima, M. Shirai, T. Ebina, M. Arai, J. Mol. Catal. A: Chem. 180 (2002) 259.
[18] M. Burgener, R. Furrer, T. Mallat, A. Baiker, Appl. Catal. A 268 (2004) 1.
[19] F. Zhao, Y. Ikushima, M. Arai, J. Catal. 224 (2004) 479.

[20] U.K. Singh, M.A. Vannice, AIChE J. 45 (1999) 1059.
[21] R.L. Augustine, P. Techasauvapak, J. Mol. Catal. 87 (1994) 95.
[22] S.-I. Fujita, S. Akihara, F. Zhao, R. Liu, M. Hasegawa, M. Arai, J. Catal. 236 (2005) 101.
[23] M. Besson, P. Gallezot, Catal. Today 81 (2003) 547.
[24] F. Zhao, K. Murakami, M. Shirai, M. Arai, J. Catal. 194 (2000) 479.
[25] F. Zhao, M. Shirai, Y. Ikushima, M. Arai, J. Mol. Catal. A 180 (2002) 211.
[26] C. Reichardt, Solvents and Solvent Effects in Organic Chemistry, 3rd ed., Wiley–VCH, Weinheim, 2003.

เอกสารแนบ 3

Available online at www.sciencedirect.com
ScienceDirect
Journal of Molecular Catalysis A: Chemical 261 (2007) 29–35
JOURNAL OF MOLECULAR CATALYSIS A: CHEMICAL
www.elsevier.com/locate/molcata

Impact of palladium silicide formation on the catalytic properties of Pd/SiO_2 catalysts in liquid-phase semihydrogenation of phenylacetylene

Joongjai Panpranot[a,*], Kunnika Phandinthong[a], Terachai Sirikajorn[a], Masahiko Arai[b], Piyasan Praserthdam[a]

[a] *Center of Excellence on Catalysis and Catalytic Reaction Engineering, Department of Chemical Engineering, Faculty of Engineering, Chulalongkorn University, Bangkok 10330, Thailand*
[b] *Division of Chemical Process Engineering, Graduate School of Engineering, Hokkaido University, Sapporo, Japan*

Received 18 May 2006; received in revised form 19 July 2006; accepted 19 July 2006
Available online 1 September 2006

Abstract

In this study, palladium silicide was formed on the sol–gel derived SiO_2 supported Pd catalysts when they were prepared by ion-exchange method using $Pd(NH_3)_4Cl_2$ as a palladium precursor. No other palladium phases (PdO or Pd^0) were evident after calcinations at 450 °C for 3 h. The Pd/SiO_2 catalysts with Pd silicide formation were found to exhibit superior performance than commercial SiO_2 supported ones in liquid-phase semihydrogenation of phenylacetylene. From XPS results, the binding energy of Pd 3d of palladium silicide on the Pd/SiO_2 catalyst shifted toward larger binging energy, indicating that Pd is electron deficient. This could probably result in an inhibition of a product styrene on the Pd surface and hence high styrene selectivities were obtained at high phenylacetylene conversions. The formation of Pd silicide, however, did not have much impact on specific activity of the Pd catalysts since the TOFs were quite similar among the various catalysts with or without palladium silicides if their average particle sizes were large enough. The TOFs decreased by an order of magnitude when palladium dispersion was very high and their average particle sizes were smaller than 3–5 nm.

Keywords: Palladium silicide; Pd/SiO_2; Sol–gel silica; Liquid-phase hydrogenation; Phenylaccetylene

1. Introduction

Pd/SiO_2 is one of the most frequently studied catalysts for liquid-phase alkyne semihydrogenation [1–8]. It is also commercially attractive for industrial applications due to its easy preparation procedure and low separation problem compared to colloidally dispersed ones. SiO_2 is a common support and known to be more inert than several reducible metal oxides such as TiO_2 or CeO_2 [9]. However, Pd–SiO_2 interaction can occur under certain cases, e.g., high temperature treatment in the presence of H_2 [10,11]. This transformation has been shown to alter the catalytic behavior of reduced Pd/SiO_2 catalysts. For example, in catalytic conversion of 2,2-dimethylbutane, formation of palladium silicides lowered the catalytic activity, decreased the activation energy, and increased the selectivity toward isomerization reaction [10]. Although metal silicide formation seemed to be a problem in catalysis on supported metal, there has been a number of studies reporting the application of palladium silicon alloy in catalytic reactions [12–14]. For instance, Baiker and coworkers [14] reported that the amorphous glassy alloy $Pd_{81}Si_{19}$ prepared by melt spinning was suitable for semihydrogenation of a propargylic alcohol and exhibited more than 50 times higher turnover frequency than a conventional silica-supported palladium catalyst under similar conditions.

In this study, palladium silicide was formed on sol–gel derived nano-SiO_2 supported Pd catalysts via a simple ion-exchange method. No high temperature reduction treatment was required for such formation. The catalysts were investigated by means of N_2 physisorption, CO pulse chemisorption, X-ray diffraction (XRD), transmission electron microscopy (TEM), and X-ray photoelectron spectroscopy (XPS). The effects of preparation method as well as the type of silica support on the characteristics and catalytic properties of Pd/SiO_2

* Corresponding author. Tel.: +66 2218 6878; fax: +66 2218 6877.
E-mail address: joongjai.p@eng.chula.ac.th (J. Panpranot).

1381-1169/$ – see front matter © 2006 Elsevier B.V. All rights reserved.
doi:10.1016/j.molcata.2006.07.053

were extensively investigated in selective hydrogenation of phenylacetylene in a liquid–solid–gas system.

2. Experimental

2.1. Catalyst preparation

Silica was prepared by the sol–gel technique using the sol composition of 40 ml of tetraethylorthosilicate (TEOS), 10.5 ml of ethanol, 12.5 ml of de-ionized water, and 1 ml of hydrochloric acid (HCl). The mixtures were stirred vigorously for 1 h. Then the gel was calcined at 500 °C for 6 h in order to remove any organic. For comparison purposes, commercial silica was large-pore silica obtained from Strem Chemicals. The Pd/SiO_2 catalysts with ca. 1 wt.% of Pd were prepared by ion-exchange and impregnation methods. For the ion-exchange method, a desired amount of $Pd(NH_3)_4Cl_2$ (Aldrich) was dissolved in deionized water. The pH of solution was adjusted to 12 using 25% NH_3 solution (Aldrich). The precursor solution was added to the silica and stirred vigorously for 3 days. The residue solid was filtered and washed with distilled water until the pH was 7. For incipient wetness impregnation method, the silica support was impregnated with an aqueous solution containing certain amount of palladium. The catalyst samples were dried in oven at 100 °C and calcined in air at 450 °C for 3 h prior to characterization.

2.2. Catalyst characterization

The BET surface areas, pore volumes, and average pore diameters were determined by N_2 physisorption using a Micromeritics ASAP 2000 automated system. Each sample was degassed under vacuum at <10 μmHg in the Micromeritics ASAP 2000 at 150 °C for 4 h prior to N_2 physisorption. The XRD patterns of the catalysts were measured from 20 to 80° 2θ using a SIEMENS D5000 X-ray diffractometer and Cu Kα radiation with a Ni filter. Catalyst crystallite sizes and diffraction pattern of silica supports were obtained using the JEOL JEM 2010 transmission electron microscope that employed a LaB_6 electron gun in the voltage range of 80–200 kV with an optical point to point resolution of 0.23 nm. The amounts of CO chemisorbed on the catalysts were measured using a Micromeritic Chemisorb 2750 automated system attached with ChemiSoft TPx software at room temperature. Prior to chemisorption, the sample was reduced in a H_2 flow at 500 °C for 2 h and then cooled down to ambient temperature in a He flow. The XPS analysis was performed using an AMICUS photoelectron spectrometer equipped with a Mg Kα X-ray as a primary excitation and a KRATOS VISION2 software. XPS elemental spectra were acquired with 0.1 eV energy step at a pass energy of 75 kV. The C 1s line was taken as an internal standard at 285.0 eV.

2.3. Reaction study

Liquid-phase semihydrogenation of phenylacetylene was carried out in a 50 cm^3 stainless steel autoclave. Approximately 0.1 g of Pd/SiO_2 catalyst was placed in the reactor with 1 cm^3 of phenylacetylene and 9 cm^3 of ethanol (Aldrich). Afterward the reactor was filled with hydrogen at 1 bar pressure. Stirring was switched on to start the reaction and carried out for 1 h. The products were analyzed by gas chromatography with flame ionized detector.

3. Results and discussion

3.1. Catalyst characterization

3.1.1. TEM with electron diffraction mode

Transmission electron micrographs and electron diffraction patterns of the two types of the SiO_2 used in this study namely SiO_2-SG (sol–gel derived silica) and SiO_2-com (commercial silica) are shown in Fig. 1. The TEM images revealed that the commercial silica is composed of many small particles with an average particle size of ca. 17 nm while larger particle size was seen for the sol–gel derived silica. However, sol–gel method usually produces single crystalline oxides, the large particles observed maybe the secondary particles formed by agglomeration of the primary nano-particles due to heat treatment during calcination step. Electron diffraction pattern of the commercial silica is clear indicating that it is totally amorphous while that of the sol–gel derived silica indicated semi-polycrystalline structure.

3.1.2. N_2 physisorption

The BET surface areas, the pore volumes, and the average pore diameters of the silica and the silica-supported Pd catalysts are shown in Table 1. The catalysts were termed Pd/SiO_2-x-im and Pd/SiO_2-x-ion according to the two preparation methods used where x = sol–gel derived (SG) or commercial SiO_2 (com). The N_2 adsorption–desorption isotherms of the sol–gel derived nano-silica and the commercial silica (not shown) indicate a typical type IV isotherm with a sharp inflection at relative pressure $P/P_0 > 0.3$, characteristics of capillary condensation. After Pd loading by the impregnation method, the BET surface areas and pore volumes slightly decreased (less than 20%) indicating that only a small amount of Pd was deposited in the pores of the silica. In contrast, the BET surface areas and pore volumes of the Pd/SiO_2 catalysts prepared by ion-exchange method dramatically decreased (~95%). Such results suggest that pore blockage or destruction of the silica pore structure occurred in such cases. There were no changes in the average pore diameters of both types of silica when the catalysts were prepared by impregnation method. It did appreciably change for those prepared by ion-exchange method.

3.1.3. X-ray diffraction

The XRD patterns of the various Pd/SiO_2 catalysts prepared by impregnation and ion-exchange method in the calcined state are shown in Fig. 2. The XRD characteristic peaks for PdO at 2θ (°) = 33.8, and less so at 42.0, 54.8, 60.7, and 71.4 were evident only for the catalysts prepared by impregnation method with Pd/SiO_2-SG-im exhibited higher peak intensities. The average PdO crystallite sizes on SiO_2-SG-im and SiO_2-com-im

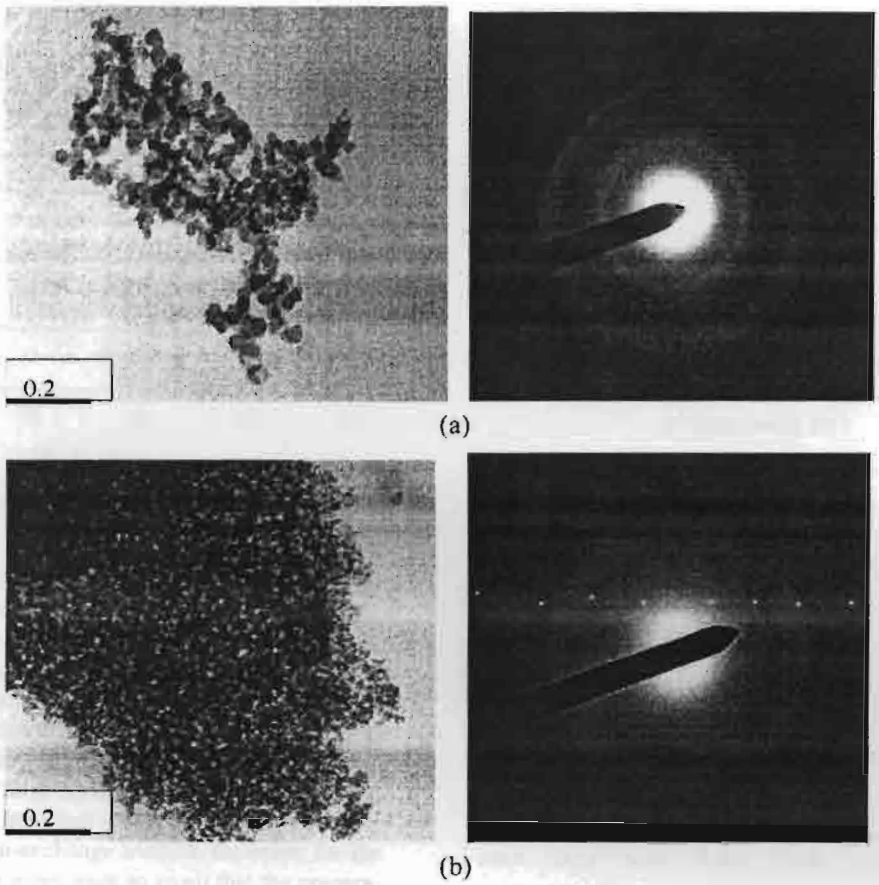

Fig. 1. TEM micrographs and diffraction patterns of (a) SiO_2-SG and (b) SiO_2-com.

were calculated from the full width at half maximum of the XRD peak at $2\theta = 33.8°$ using Scherrer equation to be 9.6 and 11.4 nm, respectively (Table 2). For the catalysts prepared by ion-exchange method, it was found that palladium silicide was formed on the sol–gel derived silica as indicated by the major XRD characteristic peak for Pd_4Si at $2\theta = 18.1°$. The average crystallite size of palladium silicide was calculated to be ca. 60 nm. It should be noted that there was no XRD characteristic peak of palladium silicide for the commercial silica supported Pd catalyst prepared by the ion-exchange method. In such case, Pd was probably highly dispersed and its average particle size was smaller than the detectability limit of the XRD (3–5 nm).

3.1.4. Surface analysis by XPS

Because of its surface sensitivity, XPS is used to identify the surface compositions of the catalysts as well as the interaction between Pd and the silica supports. The percentages of atomic concentration for Si 2p, O 1s, and Pd 3d are given in Table 2. There was a significant difference in the atomic ratios of Si/Pd for the sol–gel derived silica supported Pd catalysts prepared by impregnation and ion-exchange methods (19 and 215, respectively). While those for the commercial silica supported ones were ca. 300 and 400 for the ones prepared by impregnation and ion-exchange, respectively. The low Si/Pd ratio found for Pd/SiO_2-SG-im catalyst suggests that large amount of palladium

Table 1
N_2 physisorption results

Sample	N_2 physisorption		
	BET surface area (m^2/g)	Pore volume (cm^3/g)	Average pore diameter (nm)
SiO_2-SG	307.2	0.145	1.9
SiO_2-com	243.8	1.060	17.4
Pd/SiO_2-SG-im	248.0	0.118	1.9
Pd/SiO_2-com-im	234.0	1.017	17.3
Pd/SiO_2-SG-ion	6.2	0.009	5.9
Pd/SiO_2-com-ion	5.5	0.041	29.5

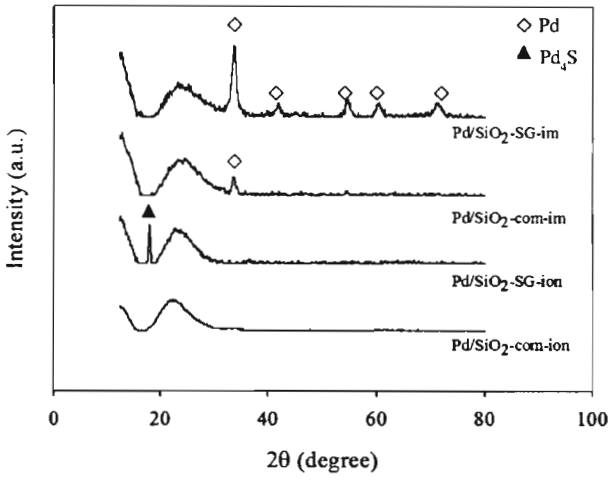

Fig. 2. XRD patterns of the various SiO_2 supported Pd catalysts.

existed on the outside of the support surface and not in the pores; the results were consistent with the N_2 physisorption results that the average pore diameters remained unaltered (~1.9 nm before and after Pd impregnation). The higher Si/Pd ratios for the other catalysts suggest that most of the palladium existed deep inside the pore of the supports rather than on the outer surface. This could be the case for the large pore commercial silica supported ones since the pores were large enough so that the solution of Pd precursor could easily be absorbed during the preparation using either impregnation or ion-exchange method. However, for the sol–gel derived silica, the pores were so small that the preparation solution could hardly penetrate these pores. The enrichment of Si component on the surface of the Pd/SiO_2-SG-ion was due to palladium silicide formation as shown earlier in its XRD pattern. A large number of the Si/Pd atomic ratio due to palladium silicide formation has also been reported for amorphous $Pd_{81}Si_{19}$ alloy catalysts [13].

The elemental scans for each component on the surfaces of the SiO_2 and the SiO_2 supported Pd catalysts prepared by impregnation and ion-exchange are shown in Figs. 3–5, respectively. For the silica supports, it was found that the binding energies of both Si 2p and O 1s for the sol–gel derived SiO_2 shifted towards lower binding energies. This suggest that on the sol–gel derived SiO_2 the Si–O–Si matrix may become the non-stoichiometric SiO_x ($0 < x < 2$) upon preparation by sol–gel technique and subsequent calcinations at high temperature. These defective sites of the SiO_2 have been found to lower the binding energy of

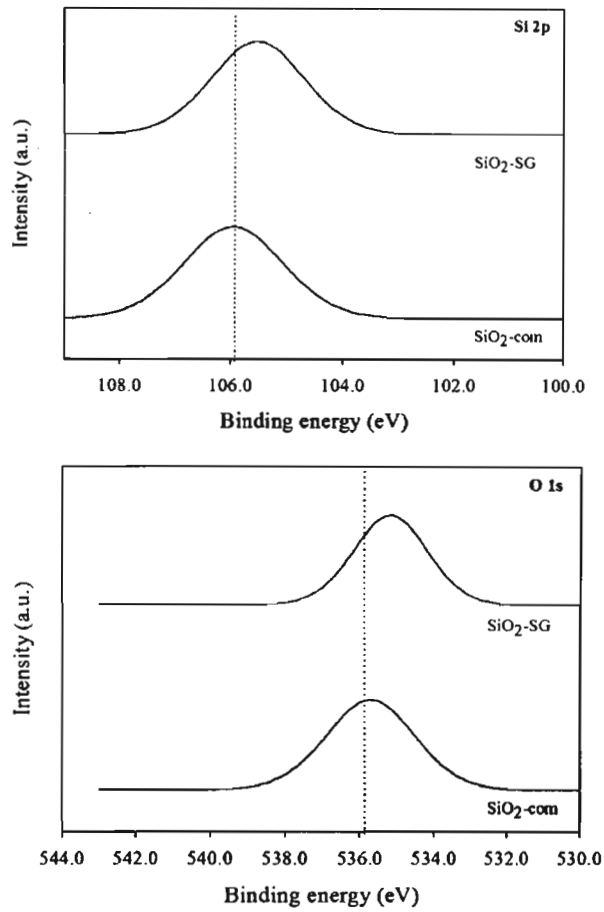

Fig. 3. XPS results of SiO_2-SG and SiO_2-com.

both Si 2p and O 1s [15]. For the Pd/SiO_2 catalysts prepared by impregnation method, there were no changes for the binding energies of Si 2p and O 1s for both Pd/SiO_2-SG-im and Pd/SiO_2-com-im. The binding energies of Pd 3d for both catalysts were also identical. Such results indicate that there was no interaction between Pd and the SiO_2 supports when the catalysts were prepared by impregnation method. On the other hand, for those prepared by ion-exchange method, the binding energies of Si 2p, O 1s, and Pd 3d for Pd/SiO_2-SG-ion shifted towards higher binding energies while those of Pd/SiO_2-com-ion were essentially the same. It is likely that formation of palladium silicide on the Pd/SiO_2-SG-ion resulted in a stronger interaction between Pd and SiO_2.

Table 2
Catalyst characterization by XRD and XPS

Catalyst	XRD		Atomic concentration (%)			Si/Pd
	Phase	Crystallite size (nm)	Si 2p	O 1s	Pd 3d	
Pd/SiO_2-SG-im	PdO	9.6	24.06	74.49	1.45	19.40
Pd/SiO_2-com-im	PdO	11.4	21.44	78.49	0.07	306.22
Pd/SiO_2-SG-ion	PdSi	61.2	25.80	74.09	0.12	215.00
Pd/SiO_2-com-ion	n.d.	n.d.	28.21	71.60	0.08	403.02

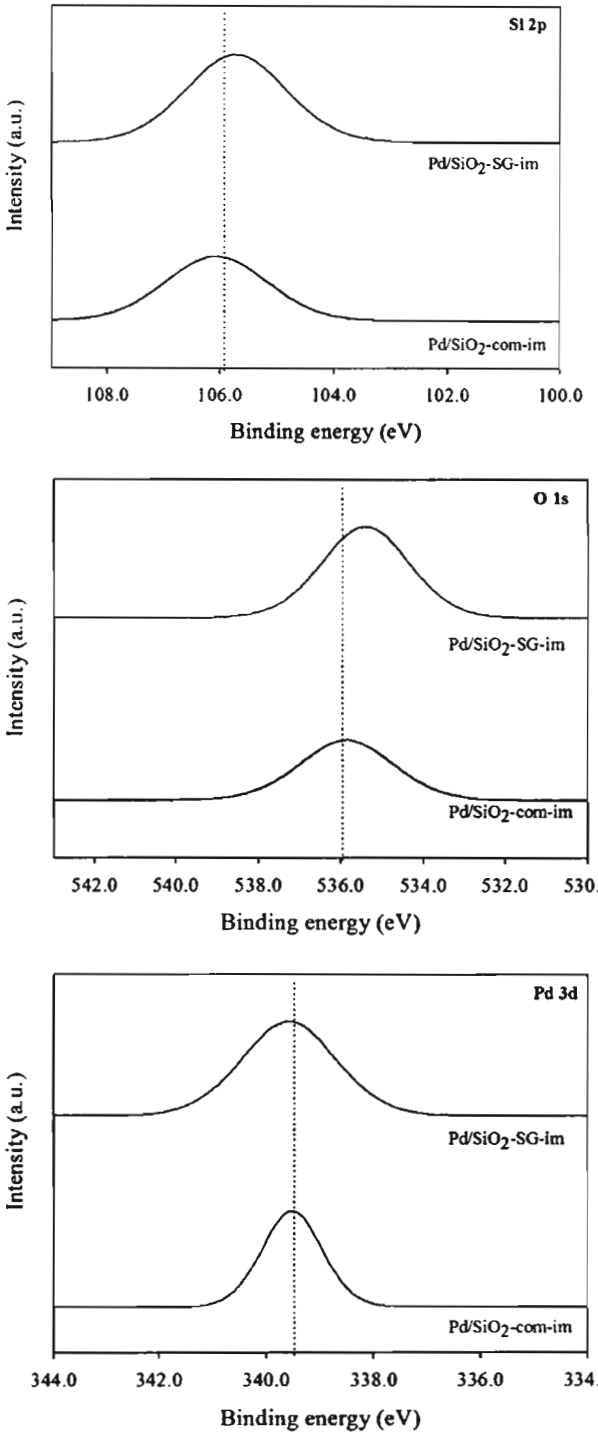

Fig. 4. XPS results of Pd/SiO_2-SG and Pd/SiO_2-com prepared by impregnation method.

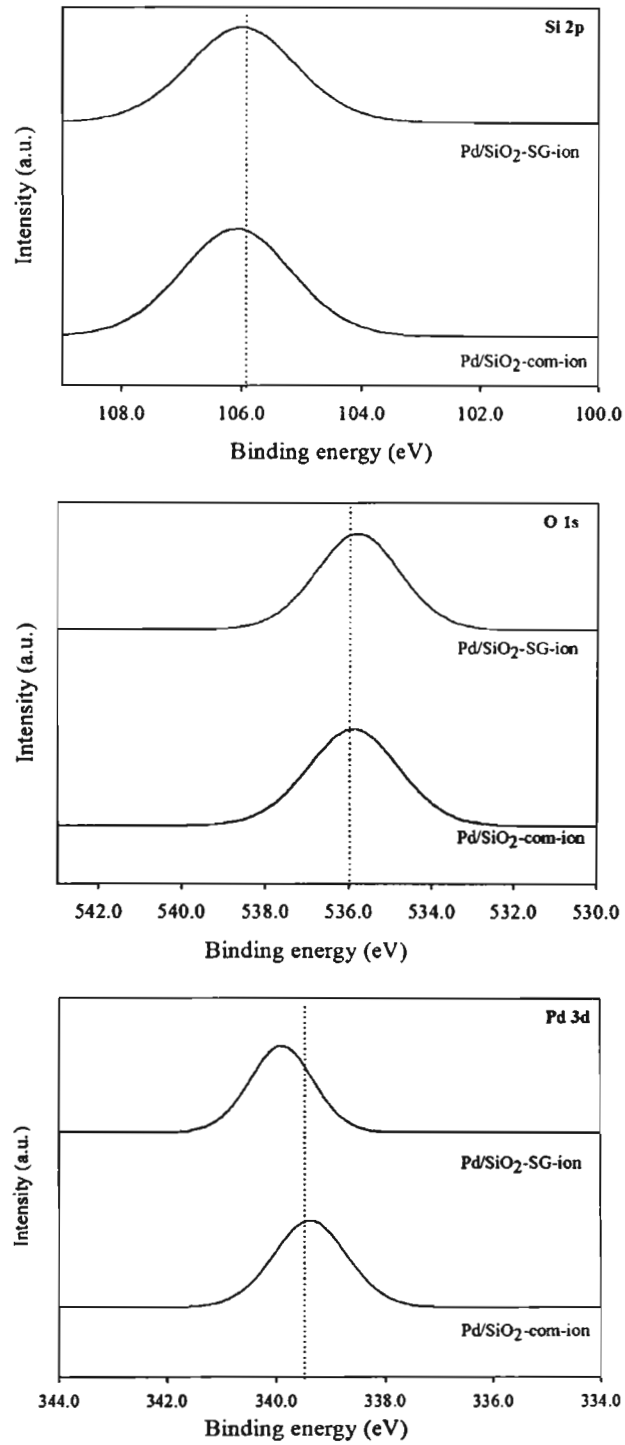

Fig. 5. XPS results of Pd/SiO_2-SG and Pd/SiO_2-com prepared by ion-exchange method.

3.2. *Proposed mechanism for palladium silicide formation*

Palladium silicides exist in various compositions such as Pd_2Si [16], Pd_3Si [11,17,18], Pd_4Si [18,19], or Pd_5Si [17]. Most of Pd silicide formation for Pd/SiO_2 catalysts reported in the literature resulted from a high temperature reduction treatment (450 °C and above) in the presence of hydrogen [13,14]. The mechanism of Pd-silicon interactions generated by high temperature reduction proposed by Karpinski and coworkers [18] involved incorporation of silicon into a palladium phase, not

Table 3
CO chemisorption results and catalyst activity in selective phenylacetylene hydrogenation

Catalyst	CO chemisorption ($\times 10^{-18}$ molecule CO/g_{cat})	Conversion[a] (%)	Selectivity[a] (%)		TOFs[b] (s^{-1})
			Styrene	Ethylbenzene	
Pd/SiO_2-SG-im	7.41	51.1	96.0	4.0	1.20
Pd/SiO_2-com-im	3.32	31.2	91.1	8.9	1.61
Pd/SiO_2-SG-ion	3.92	40.1	92.9	7.1	1.74
Pd/SiO_2-com-ion	46.8	54.8	88.5	11.5	0.20

[a] The reaction conditions were H_2 1 bar, 30 °C, and reaction time 1 h.
[b] Based on CO chemisorption results.

vice versa. Reduction of Pd/SiO_2 at high temperature initially resulted in Pd_4Si formation which was then further reacted with silicon species to a Pd_3Si phase. Other possible mechanisms involved diffusion of Si through a thin layer of Pd to the surface [20–22]. However, in this study, formation of palladium occurred during preparation of sol–gel derived silica supported Pd catalysts by ion-exchange method following calcination at 450 °C for 3 h. The use of commercial amorphous SiO_2 did not result in such formation. Based on the work of Ichinohe et al. [15] about palladium silicide formation in Pd/SiO_2 complex films, it is believed that oxygen vacancies are the primary diffusion pathways for the formation of silicide at the interface between SiO_2 and Si. Point defects on SiO_2 thin film has been reported as the primary mechanism for inter-diffusion of Pd. Deposition of elemental Si on Pd on less defective SiO_2 thin film does not produce a silicide feature. The results in this study are in good agreement with those reports that palladium silicide formation was initiated from the defective sites of the SiO_2 since the sol–gel derived SiO_2 contained more defective sites than the commercial ones (as shown by a shift of the XPS Si 2p peak toward lower binding energy).

3.3. Catalyst activity in liquid phase hydrogenation of phenyl acetylene

Table 3 shows the CO chemisorption results, the activity and the selectivity of the catalysts in liquid phase hydrogenation of phenyl acetylene, and the calculated turnover frequencies (TOF). The effect of Pd dispersion on the alkyne hydrogenation has been widely studied and it is well known that changes in metal dispersion, i.e. different particle sizes lead to changes in TOF and selectivity. Since the catalyst activities/conversions in this study (e.g. for Pd/SiO_2-SG-ion and Pd/SiO_2-com-ion) did not correlate with the CO chemisorption results and only TOF was changed significantly. This indicates that the specific activity of such catalysts depends on the Pd particle size and the reaction may be a structure-sensitive reaction. Such results, however, were found to be in agreement with the well-established trend in the literature that the specific activity decreases as metal particle size decreases [23–29]. The difference becomes significant when the average Pd particle size is very small (<3–5 nm).

Overall, the selectivity for styrene of the sol–gel derived silica supported Pd catalysts was higher than those of the commercial silica supported ones regardless the preparation method used. From the performance curves of all the catalysts (Fig. 6), the

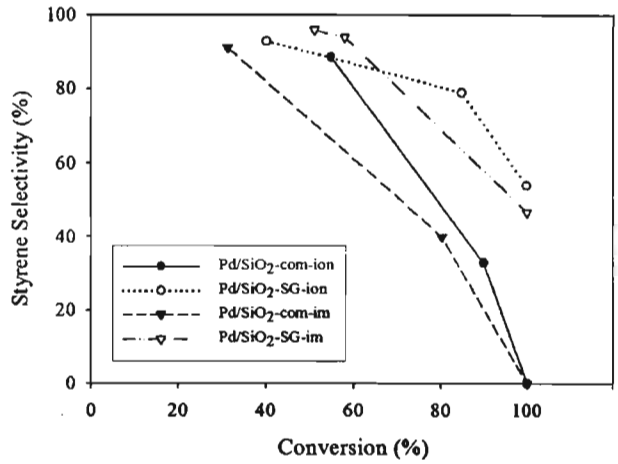

Fig. 6. Performance curves of Pd/SiO_2-SG and Pd/SiO_2-com catalysts.

sol–gel derived silica supported Pd catalysts prepared by ion-exchange and impregnation method exhibited relatively high styrene selectivity at 100% conversion of phenylacetylene with the one containing palladium silicide exhibited the highest selectivity. Under similar conditions, the commercial supported catalysts (both Pd/SiO_2-com-im and Pd/SiO_2-com-ion) exhibited no styrene selectivity at all. A possible explanation is an inhibition of a product of styrene, which is adsorbed on the surface of Pd, more strongly on Pd/SiO_2-SG in which Pd is electron-deficient (larger binding energy from XPS results). Additional hydrogenation reaction experiments with only styrene and the mixture of styrene and phenylacetylene were carried out in order to confirm the hypothesis. It was found that the commercial silica supported Pd catalysts exhibited higher styrene conversion than the sol–gel derived silica supported ones during hydrogenation of only styrene. Higher ethylbenzene selectivities were also observed for the commercial silica supported catalysts during hydrogenation of the mixture of styrene and phenylacetylene suggesting that styrene hydrogenation occurred on such catalysts.

4. Conclusions

It was revealed by XRD and XPS analysis that palladium silicide was formed on the sol–gel derived silica supported Pd catalysts prepared by ion-exchange method. However, such catalysts exhibited good performances in liquid-phase

semihydrogenation of phenylacetylene with highest styrene selectivity (~60%) at 100% conversion of phenylacetylene while the commercial SiO_2 supported ones exhibited no styrene selectivity. The specific activity of the catalysts was not affected by the formation of palladium silicide since the TOFs were essentially the same regardless of palladium silicide formation. They were rather influenced by the changes in palladium particle size since the TOFs decreases by an order of magnitude when palladium particle sizes were smaller than 3–5 nm.

Acknowledgments

Authors would like to thank the Thailand Research Fund (TRF), the Graduate School of Chulalongkorn University, and the Commission for Higher Education for the financial supports.

References

[1] L. Guczi, A. Horvath, A. Sarkany, Stud. Surf. Sci. Catal. 145 (2003) 351.
[2] O. Dominguez-Quintero, S. Martinez, Y. Henriquez, L. D'Ornelas, H. Krentzien, J. Osuna, J. Mol. Catal. A 197 (2003) 185.
[3] I. Palinko, Appl. Catal. A 126 (1995) 39.
[4] T. Lopez, M. Asomoza, P. Bosch, E. Garcia-Figueroa, R. Gomez, J. Catal. 138 (1992) 463.
[5] T. Nozoe, K. Tanimoto, T. Takemitsu, T. Kitamura, T. Harada, T. Osawa, O. Takayasu, Solid State Ionics 141 (2001) 695.
[6] J.W. Park, Y.M. Chung, Y.W. Suh, H.K. Rhee, Catal. Today 93 (2004) 445.
[7] N. Marin-Astorga, G. Pecchi, J.L.G. Fierro, P. Reyes, Catal. Lett. 91 (2003) 115.
[8] D.V. Nadkarni, J.L. Fry, J. Chem. Soc., Chem. Commun. 12 (1993) 997.
[9] G.L. Haller, D.E. Resasco, Adv. Catal. 36 (1989) 173.
[10] W. Juszczyk, Z. Karpinski, D. Lomot, J. Pielaszek, J. Catal. 220 (2003) 299.
[11] W. Juszczyk, D. Lomot, J. Pielaszek, Z. Karpinski, Catal. Lett. 78 (2002) 95.
[12] A. Molnar, G.V. Smith, M. Bartok, J. Catal. 101 (1986) 67.
[13] R. Tschan, R. Wandeler, M.S. Schneider, M. Burgener, M.M. Schubert, A. Baiker, J. Catal. 204 (2001) 219.
[14] R. Tschan, R. Wandeler, M.S. Schneider, M. Burgener, M.M. Schubert, A. Baiker, Appl. Catal. A 223 (2002) 73.
[15] T. Ichinohe, S. Masaki, K. Kawasaki, H. Morisaki, Thin Solid Film 343 (1999) 119.
[16] R. Lamber, N. Jaeger, G. Schulz-Ekloff, J. Catal. 123 (1990) 285.
[17] W. Juszczyk, Z. Karpinski, J. Catal. 117 (1989) 519.
[18] W. Juszczyk, Z. Karpinski, J. Pielaszek, J.W. Sobczak, New J. Chem. 7 (1993) 573.
[19] L. Kepinski, M. Wolcyrz, Appl. Catal. 73 (1991) 173.
[20] B. Schleich, D. Schmeisser, W. Gopel, Surf. Sci. 191 (1987) 367.
[21] A.J. Brunner, P. Oelhafen, H.-J. Guntherodt, Surf. Sci. 188 (1987) 1122.
[22] A.J. Brunner, A. Stemmer, L. Rosenthaler, R. Wiesendanger, M. Ringer, P. Oelhafen, H. Rudin, H.-J. Guntherodt, Surf. Sci. 181 (1987) 313.
[23] N. Marin-Astroga, G. Alvez-Manoli, P. Reyes, J. Mol. Catal. A 226 (2005) 81.
[24] A. Molnar, A. Sarkany, M. Varga, J. Mol. Catal. A 173 (2001) 185.
[25] D. Duca, L.F. Liotta, G. Deganello, J. Catal. 154 (1995) 69.
[26] G. Carturan, G. Facchin, G. Cocco, S. Enzo, G. Navazio, J. Catal. 76 (1982) 405.
[27] A. Sarkany, A.H. Weiss, L. Guczi, J. Catal. 98 (1986) 550.
[28] P. Albers, K. Seibold, G. Prescher, H. Muller, Appl. Catal. A 146 (1999) 135.
[29] G. del Angel, J.L. Benitez, J. Mol. Catal. A 94 (1994) 409.